NIOZ

Royal Netherlands Institute for Sea Research

This is a pre-copyedited, author-produced version of an article accepted for publication, following peer review.

Published version: https://dx.doi.org/10.3354/meps13267

NIOZ Repository: http://imis.nioz.nl/imis.php?module=ref&refid=323729

Research data: https://dx.doi.org/10.4121/12872684

[Article begins on next page]

1 Title: Planktonic primary production in the western Dutch Wadden Sea

2 Authors: Jacobs, P, Kromkamp, JC, van Leeuwen, SM and Philippart, CJM

3

4 Abstract [maximum of 250 words]

5

6 Pelagic primary production measurements provide fundamental information about the

7 trophic status of a marine ecosystem. Measured carbon-fixation rates generally have a

8 limited temporal and spatial resolution, but can be combined with Earth Observation

9 data to extrapolate the measurements. Here, production-irradiance curves were fitted

10 for three years of ^{14}C incubation data from the western Wadden Sea, using four different

11 models, two with and two without photo-inhibition. The curve-fit model by Jassby &

12 Platt (1976) best fitted the data. Applying this model showed that the photosynthetic

13 parameters, normalised for chlorophyll-a concentration, P^B_{max} and α^B, were correlated.

14 Seasonality in photosynthetic parameters of this model and the relationship with

15 environmental variables was explored, with a focus on variables that can be inferred

16 from satellite algorithms. There was no significant correlations between α^B and any of

17 the environmental variables measured. While P^B_{max} correlated with SST, the vertical

18 light attenuation coefficient, silicate and nitrate + nitrite concentration, the multivariate

19 model that best explained the variation in estimates of P^B_{max} was a model that included

20 SST and year. In the period from 2012 to 2014, daily and annual production ranged

21 between 3.4 - 3800 mg C d^{-1} and between 131-239 g C m^{-2} y^{-1} respectively. Comparison

22 of the results with historical data (1990-2003), indicated that the decline in planktonic

23 primary production since the 1990s has halted. Although not tested, we believe that our

24 approach is generally applicable to coastal waters.

1

2

3

1. Introduction

Measurements of planktonic primary production provide fundamental information about the trophic status of marine ecosystems (Pereira et al. 2013, Muller-Karger et al. 2018). Historically, measured carbon-fixation rates come from ^{14}C incubations (Longhurst et al. 1995). Not only are such measurements logistically difficult and expensive to sustain as part of long-term monitoring programs, these discrete measurements provide information valid for a very small spatial and temporal scale only (Behrenfeld & Falkowski 1997). Upscaling these measurements requires at least knowledge of the regional and seasonal distribution of algal biomass (Longhurst et al. 1995). Since 1978, this information is available from satellite-retrieved data (Longhurst et al. 1995, Behrenfeld & Falkowski 1997). Although progress has been made since then, such remotely sensed data is far from perfect, with poor performance due to cloud-cover, and, in coastal areas, interference of suspended matter and CDOM concentrations with satellite signals, hampering a reliable estimate of the chlorophyll-a concentration (Joint & Groom 2000, Jamet et al. 2011, Aurin & Dierssen 2012, Chen et al. 2013). On the positive side, these shortcomings are partly compensated for by the large number of observations. Satellite derived data can be combined with principles of algal physiology to potentially estimate primary production (Longhurst et al. 1995).

Light availability is a critical factor controlling primary production (Cole & Cloern 1984, 1987, Pennock & Sharp 1994, Heip et al. 1995, Cloern 1999). Estimation of annual production from a relatively few images per year is based on several assumptions, amongst others with respect to the relationship between productivity and light conditions (PE-curves).

1   Annual productivity is generally calculated as the sum of daily productivity for all days

2   of the year. Daily productivity can be derived from incubations of water samples with

3   ^{14}C during a fixed period (often one to two hours), the so-called carbon fixation rate (P),

4   at a range of light conditions (E) and the light conditions in the water column during the

5   day. These daily light conditions in the water column are determined by the daily

6   insolation at the water surface and light attenuation in the water column.

7   PE-curves have either two (in the absence of photo-inhibition) or three parameters

8   (allowing photo-inhibition) and the rates are often normalized to the chlorophyll-a

9   concentration, giving the following parameters α^B, P^B_{max} and, in case, the model includes

10 photo-inhibition, β^B. If photo-inhibition occurs, then applying a model without photo-

11 inhibition is expected to overestimate water column production (Platt et al. 1980). The

12 actual occurrence of photo-inhibition however might also be exaggerated because of too

13 long incubations at high light intensities, but the importance of this incubation artefact

14 is hard to quantify (Peterson, 1980, Grobbelaar, 1985).

15 So far, satellite images have been able to supply data on light conditions, light

16 attenuation in the water, chlorophyll-a concentrations, sea surface temperatures and

17 (more recently) salinity (Gabarro et al. 2004, Klemas 2011), but not on the parameters

18 of the photosynthetic parameters α^B, P^B_{max} and β^B. If these parameters could be derived

19 as well, this more extensive data set would allow for more extensive monitoring of

20 temporal and spatial variation such as shifts in the timing of phytoplankton blooms,

21 gradients in pelagic production in river outflows and trends in overall productivity

22 (Pereira et al. 2013). Modelling of photosynthetic parameters as a function of

23 temperature (Behrenfeld & Falkowski 1997, Cox et al. 2010) or of temperature and

1   nutrients (Cox et al. 2010) would allow for indirect estimates of pelagic production from

2   satellite data.

3   In this paper, PE-parameters derived from 2h incubations in a photosynthetron are

4   used to estimate daily and annual productivity. Four different models are applied and

5   the effect of model choice on the estimated productivity is compared. Using the best

6   model for the dataset, seasonality in the photosynthetic parameters and the

7   relationships between the values of these parameters with environmental conditions

8   (daily insolation, SST, salinity, turbidity, concentrations of nutrients and chlorophyll-a)

9   is explored. This analysis is based upon three years (2012-2014) of ^{14}C incubation data

10   derived from the Marsdiep, the westernmost tidal inlet of the Wadden Sea, a shallow

11   subsystem separated from the North Sea (northern Europe) by a chain of barrier

12   islands. This area was subject to eutrophication in the mid-1970s, followed by a

13   reduction in nutrient supply since the late 1980s (Philippart et al. 2000). These changes

14   in trophic states were reflected in changes in biomass, species composition and

15   production of phytoplankton (Philippart et al. 2000, 2007). Annual production rates of

16   2012-2014 were compared with data from 1990-2003 (Philippart et al. 2007) to

17   explore if the previously described decline had persisted.

18

19

1 ## 2. Material and Methods

2

3 *2.1 Data collection*

4 Water samples were collected at high tide from the NIOZ-jetty (53°00′06″ N; 4°47′21″

5 E) in the Marsdiep tidal basin (Figure 1). The depth at the sampling location is 3m, while

6 the average depth in the Marsdiep tidal basin is 4.6m (Ridderinkhof 1988, Cadée &

7 Hegeman 2002). The samples were taken with a bucket, 40 times a year with an average

8 frequency of once a week from March to September and approximately twice a month

9 from October to February. Water temperature (SST; °C) was measured directly using a

10 bucket thermometer (unknown brand and type, accuracy 0.1°C), salinity (PSU) was

11 measured by reading the refraction index of 0.2μm-filtered seawater that was

12 acclimatised to laboratory temperature using a handheld refractometer (ENDECO type

13 102, accuracy 0.1‰). The refraction index (or salinity) was then corrected for

14 temperature using temperature-salinity charts. Chlorophyll-a concentrations were

15 determined by filtering 250-500 ml water over Whatman GF/F filters (47mm diameter),

16 filters were quick-frozen in liquid nitrogen and subsequently stored at -80°C until

17 analyses. Samples were analysed within one year by high-performance liquid

18 chromatography (HPLC) according to Evans et al. (1975). Total dissolved inorganic

19 carbon (DIC) was measured by potentiometric titration. The underwater light

20 attenuation (k_d) can be derived directly using two spherical underwater quantum

21 sensors 'PAR$_1$' and 'PAR$_2$' (LI-COR LI-193), which were placed at 1.55 (the highest

22 distance possible due to tidal height) and 2.05 meter depth at the jetty:

23 $$k_d = \ln\left(\frac{PAR_1}{PAR_2}\right)/z$$

1   Due to the relative turbidity of the area, the sensors were placed at a relatively short

2   distance from each other. This distance has proven to allow for accurate estimates of k_d.

3   Data from these two PAR sensors was available only for part of 2014 and 2015. For the

4   period of interest, 2012-2014, only Secchi disk depths (Z_{SD}; m) were available

5   throughout. Therefore, first an empirical relation between k_d and Z_{SD} was derived

6   following the theoretical relation by Holmes (1970), using data from 2014 and 2015:

7
$$k_d = \frac{a}{Z_{SD}} + b$$

8   With a = 1.476 [-] and b = 0.3541 [-]. The value of a is within the range found for other

9   coastal waters (Lee et al. 2018). This relationship (n = 40, r^2 = 0.63) was used to

10   estimate light attenuation from Secchi-disk depth for all sampling dates in the period

11   2012-2014 in the Marsdiep area.

12   Mixing depth (Z_{mix}; m) is set equal to the average depth of the Marsdiep basin (4.6m)

13   since the water column is mixed for most of the time (Nauw et al. 2014) and the

14   euphotic depth (Z_{eu}; m), is defined as the depth at which 1 % of the light measured at

15   the surface penetrated: $(\frac{\ln\left(\frac{100}{1}\right)}{K_d})$.

16   Hourly values of irradiance (PAR) just above the water surface (E_{PAR+0}; µmol photons

17   m^{-2} h^{-1}; 400-700nm) were measured at the jetty (TriOS RAMSES ACC). In case of missing

18   values, data on average hourly irradiance (E_0; J cm^{-2}) were taken from the KNMI station

19   at the "De Kooy" airport (Figure 1) and converted to µmol photons m^{-2} s^{-1} PAR using an

20   empirical relation derived by comparing light measurements from the sensor at the

21   jetty to data from "De Kooy" station (n=8760, r^2=0.94) (E_{PAR+0} = E_0 x 5.95).

22   Samples for dissolved inorganic nutrients analysis were filtered over a 0.22µm

23   polycarbonate filter and stored until analysis at -20°C for N and P or 4°C for Si. Nutrient

1   concentrations were analysed at the NIOZ using a Traacs 800 auto-analyser

2   (Technicon). To explore the variation in and correlation between environmental

3   variables a Principal Component Analysis was performed using R library 'vegan' (R Core

4   Team 2018). For all analysis R version 3.5.1 was used. Variables were normalised

5   before the analysis.

6   *2.2 Carbon fixation measurements*

7   A sample of 90 ml was spiked with 2.25 ml $NaH^{14}CO_3^-$ with an activity of approximately

8   1Mbq ml^{-1}, the sample was gently mixed and divided over 23 incubation flasks holding

9   4.1 ml each. The actual activity added per incubation was determined by measuring the

10   activity of the flask with 100 µl $NaH^{14}CO_3^-$ added to 4 ml of 1M NaOH, this flask served

11   as the 'control' and was not incubated but was closed and placed under the fume hood.

12   The 22 flasks with spiked seawater were placed in a photosynthetron (CHPT, model

13   TGC1000, equipped with two halogen light bulbs (Philips 13095, 250W)) and incubated

14   for 2 hours at *in situ* temperatures (Lewis & Smith 1983). The incubation temperature

15   was controlled by a water bath; temperatures in the incubator were measured before

16   and directly after the incubation. Despite the use of the water bath, temperatures

17   deviated from *in situ* temperatures occasionally. In those instances, a correction factor

18   T_{corr} (°C) was applied, with $T_{corr}=e^{0.0693}$ x (T $_{in\ situ}$-$T_{incubation}$). Temperature differences

19   between *in situ* and incubation (average of temperature at the start and the end) varied

20   between 0.4 and -4.2°C.

21   Two flasks of the 22 were covered with aluminium foil, receiving no light. The

22   radioactivity measured in these samples after incubation served as 'dark' values and

23   were subtracted from the samples incubated in the light.

1   Directly after incubation, 100 µl concentrated (37 %) HCl was added to each flask

2   (except the control) to halt further uptake of bicarbonate and the incubation flasks

3   remained for 24 hours under the fume hood to degas. Scintillation fluid (Ultima Gold)

4   was added and analysis of radioactivity (disintegrations per minute, dpm) was carried

5   out using a scintillation counter (PerkinElmer, Tri-Carb 2910TR).

6   Light at each position in the photosynthetron was measured inside the incubation flasks

7   using a light meter (WALZ ULM-500) with spherical micro sensor (US-SQS/L). Light

8   levels received (E_s) ranged from zero to a maximum of 1700 µmol photons m^{-2} s^{-1} (PAR)

9   depending on the position of the flask in the photosynthetron. The carbon fixation rate

10   (P;mg C $L^{-1}h^{-1}$) per sample was calculated according to:

11     $$P = \left(\frac{(dpm_{sample} - dpm_{avg\_dark}) \times DIC \times 1.05 \times T_{corr}}{dpm_{added} \times t} \right)$$

12   Here, DIC is the concentration dissolved inorganic carbon (mg L^{-1}). For sampling dates

13   in 2013 and 2014, DIC was estimated using titration (Strickland & Parson 1972). No

14   data on DIC concentrations were, however, available for 2012. For 2013 and 2014, there

15   was no clear seasonal trend, and average values did not significantly differ between

16   these two years (2013: 26.7 ± 1.0 mg L^{-1}, 2014: 25.2 ± 1.6 mg L^{-1}). Therefore, the median

17   DIC for the period 2013-2014 of 26.0 mg L^{-1} was used for all calculations in 2012, 2013

18   and 2014. In the equation, 1.05 is a correction factor for the preference of the enzyme

19   Rubisco for the ^{12}C atom over the ^{14}C atom. Furthermore, dpm_{added} is the dpm as

20   measured in the control bottle and *t* is the duration of the incubation in hours. The

21   carbon fixation rate (P; mg C L^{-1} h^{-1}) was then divided by the chlorophyll-a

22   concentration of the sample to obtain chlorophyll-specific fixation rates (P^B; mg C (mg

23   Chl)$^{-1}$ h^{-1}). Recent research has indicated that the ^{14}C method gives an approximation of

1   net production for most species (Pei & Laws, 2013). However, research by Halsey et al.

2   (2010, 2013, Milligan et al. 2015) clearly demonstrates that the growth rate of the algae

3   is the factor that determines if short term incubations measure net or gross

4   photosynthesis (or something in between).

5   *2.3 PE- curve fitting*

6   Fixation rates (P^B) were used to construct PE- curves and to estimate the

7   photosynthetic parameters from the curves according to four models, being those by

8   Eilers & Peeters (1988)(EP), Jassby & Platt (1976)(JP), Platt, Gallegos & Harrison

9   (1980)(PGH) and Webb et al. (1974)(Webb). Although these models originally use

10   different functions and defining parameters, similar photosynthetic parameters can be

11   derived for the models excluding photo inhibition (parameters P^B_{max}, α^B) and those

12   including photo inhibition (P^B_{max}, α^B, β^B) (Figure 2, Table 1).

13   Estimation of the photosynthetic parameters for biomass-specific carbon fixation (P^B_{max},

14   α^B) of these four models was performed by means of the R library 'phytotools'. (R Core

15   Team 2018, Silsbe & Malkin 2015). For all models, the lower limit of 0.0 for estimation

16   of the parameters (performed by phytotools) was insufficient: despite the parameters

17   being positive, small negative values were needed within the iterative process to arrive

18   at the best parameter estimation for this dataset. Thus, lower limits were adjusted to

19   -1.0. In order to compare photo-inhibition effects between the PGH and EP models the

20   photo-inhibition slope β^B (mg C L^{-1} h^{-1} (μmol m^{-2} s^{-1})$^{-1}$) was defined as the downward

21   slope between the optimal light intensity and twice the optimal light intensity (Figure

22   2). Note that a positive β^B therefore indicates that photo-inhibition is occurring.

23   In addition, the model of Eilers and Peeters (1988) has a term E_{opt} (E_{max} in Figure 2),

24   which describes the irradiance at which photosynthesis reaches it maximum value

1   before it declines again because of photo-inhibition. This model is the only one of the

2   four models used in the current paper that is based on a mechanistic description of the

3   photosynthetic process. The photosynthetic parameters α and P_{max} are derived from the

4   fit-coefficients a, b and c. The EP model has been reformulated by Herlory et al. (2007)

5   so that the fit-parameters α and P_{max} can be derived directly from the PE-data (Table 1).

6   In the PGH model, P_s equals P_{max} when there is no photo-inhibition ($\beta^B=0$). If $\beta^B>0$, then

7    $P_s>P_{max}$, and P_s can be interpreted as the "maximum photosynthesis output that could be

8   sustained if there were no β." (Platt et al. 1980). Parameters $E_K =P_{max}/\alpha$ (Talling 1957)

9   is the saturating irradiance, the inflection point where photosynthesis becomes

10   saturated (Figure 2). This parameter gives an indication of the light-shade adaptation

11   characteristics (Falkowski & Raven 2007) and estimated values for E_k provide

12   information on the light acclimation status of the phytoplankton community.

13   The results of the curve fits were compared between models based on the smallest

14   squared sum of the residuals (ssr) (Spiess & Neumeyer 2010). Because the models

15   including photo-inhibition are more complex (three photosynthetic parameters) than

16   the ones without (two photosynthetic parameters), model selection was also done by

17   using the Akaike Information Criterion (AIC), which deals with the trade-off between

18   the goodness of fit of the model and its simplicity (Burnham & Anderson 2004).

19   Covariance between the estimates of the photosynthetic parameters was checked by

20   means of Pearson correlation. The results of the model that gave the best fit were used

21   to explore possible reasons for the observed seasonal and year-to-year variation in the

22   photosynthetic parameters.

23

1   *2.4 Calculation of daily and annual production*

2   Daily production estimates for the water column (mg C m^{-2} d^{-1}) for sampled days were

3   based upon the photosynthetic parameters from all four models, hourly values of

4   irradiance in PAR (from the jetty and, in case of missing values, from the nearest KNMI

5   station "De Kooy") and light attenuation in the water column. Maximum water depth for

6   which the production was calculated was fixed at 4.6m. Irradiance in the water column

7   just under the water surface (E_{PAR-0}; µmol photons m^{-2} h^{-1}) was corrected for reflectance

8   at the water surface (7 %; Højerslev 1978, cf. Philippart et al. 2007). Daily estimates of

9   primary production were made using the 'phytotools' package (R Core Team 2018,

10 Silsbe & Malkin 2015, this paper) by integration of the fitted curve over depth and time

11 (24 hours). Primary production on non-sample days was calculated in the same way,

12 using observed hourly irradiance values together with linearly interpolated values for

13 the vertical light attenuation (K_d; m^{-1}), chlorophyll-a concentration (µg Chl L^{-1}) and

14 photosynthetic parameters (P^B_{max}, α^B, and possibly β^B). Thus, an estimation was made of

15 the PE-curve parameters on a non-sample day based on the curve parameters of the

16 surrounding sample days, thus defining the PE-curve used for integration to daily

17 primary production on the non-sample day. The annual production (g C m^{-2} y^{-1}) was

18 estimated by adding up all daily primary production values of the year (including a leap

19 day for 2012).

20 *2.5 Relationships between photosynthetic parameters and environmental conditions*

21 The results of the best PE-model were subsequently used to explore relationships

22 between parameter values and environmental conditions focussing on those variables

23 that can be obtained from Earth Observation data. Estimated photosynthetic

24 parameters α^B and P^B_{max} were correlated to the environmental variables and only

1 variables that were significantly correlated (p<0.05) were used in the multivariate

2 model. Three models were explored, one with year as a factor (model a), one without

3 year as a factor (model b) and one model where extreme values of the PE-parameters

4 were removed (model c). Extreme values were defined as: (values-mean) > 3 x standard

5 deviation. From the full model, variables were subsequently removed when they did not

6 significantly add to the explained variance.

7 3. Results

8

9 *3.1 Environmental conditions*

10 There were considerable differences in environmental conditions between years

11 (Figure 3A & B). The year 2013 was relatively cold, with a median sea surface

12 temperature of 11.9°C (Figure 3A) compared to 2012 (14.6°C) and 2014 (15.8°C). In

13 2013, the water temperature remained relatively low (e.g. < 5°C) until mid-April (Figure

14 4). The highest maximum water temperature of the three years was recorded in 2014

15 (22.1°C), while the highest temperature in 2012 and 2013 was 20.4 and 20.2°C

16 respectively (Figure 3A, Figure 4).

17 The timing of the onset of the spring bloom, defined as a daily increase in chlorophyll-a

18 concentration above 0.2 µg L^{-1} d^{-1} (Philippart et al. 2007) was remarkably similar in the

19 three years, with an estimated onset in the second week of March in each year (Julian

20 day 72, 71 and 69 in 2012, 2013 and 2014 respectively). Peak chlorophyll-a

21 concentrations for the spring bloom were 25.4, 21.0 and 21.5 µg L^{-1} in order of years. In

22 2012, there was a second peak in the chlorophyll-a concentration of 27.8 µg L^{-1} on day

23 194 (23 July) (Figure 5). The median concentration of phytoplankton was 4.6 µg Chl L^{-1}.

1   In 2013, the coldest year, the bloom lasted longer; there were several peaks in

2   chlorophyll-a concentration, with a maximum concentration of 55.9 µg L^{-1} on day 147

3   (27 May). The median concentration in 2013 of 7.2 µg L^{-1} was higher than in 2012, but

4   lower than in 2014 (7.8 µg L^{-1}) (Figure 3A). In 2013, the chlorophyll-a concentration

5   decreased from day 175 (24 June) onwards until day 204, when there was another

6   peak. In 2012, there was a last peak at day 194 (12 July). In 2014, a peak in summer was

7   absent. The year 2014 was the only year with a small autumn bloom (day 267, 24

8   September).

9   Attenuation coefficients (K_d) ranged from 0.88 and 4.0 m^{-1} (Figure 3A), with median

10   values highest in 2013 (1.83) compared to 2012 (1.49) and 2014 (1.67). From 2012 to

11   2014, the euphotic depth (Z_{eu}) ranged between 1.1 and 5.2 m. The ratio between Z_{eu} and

12   mixing depth (Z_{mix}) was between 0.2-1 for most sampling dates, indicating that there

13   was positive net productivity, but over a depth smaller than the average water depth.

14   Median salinity values were not so different between the years (29.4, 28.6 and 29.1

15   respectively for 2012, 2013 and 2014).

16   There were clear seasonal patterns in the nutrient concentrations (Supplement 1), with

17   the highest average concentrations in winter. The concentration of Si and PO_4 (µmol L^{-1})

18   decreased sharply from day 60 to day 90, corresponding with the time of phytoplankton

19   bloom. The concentration of dissolved nitrogen (nitrate, nitrite and ammonium (DIN),

20   µmol L^{-1}) declined as well, but with a lower magnitude. Silicate concentrations

21   remained low until September. The lowest concentration for PO_4 was found in April,

22   while for DIN lowest concentrations were found in August. Redfield ratios of nutrients,

23   combined with absolute concentrations, can provide information about the nutrient, or

24   combination of nutrients that are limiting phytoplankton biomass (Redfield, 1958). A

1　DIN:DIP ratio >16 indicates a P-limitation, while a ratio <16 indicated N-limitation.

2　However as long as concentrations exceed 21-36 µmol L^{-1} for DIN and 0.16 µmol L^{-1} for

3　DIP than neither nutrient is considered limiting (Redfield 1958, Ekholm 2008). For

4　diatoms a DIP:Si ratio above 0.07 indicates a silicate limitation (Redfield 1985 in

5　Ekholm 2008). In the current study, the Redfield ratio of DIN:DIP was found to be <16

6　occasionally in the months July to September, while the ratio of DIP: Si was above 0.07

7　from April to October. Combined with the absolute concentrations measured, it can be

8　concluded that for the years 2012-2014 at the Marsdiep jetty, nitrogen was limiting

9　phytoplankton biomass in summer, while the rest of the year there was a co-limitation

10　of DIP and silicate (Supplement 1). With regard to the differences between the years, it

11　can be seen that variation in nutrient concentrations was higher in 2013 compared to

12　the other two years (Figure 3B).

13　The results from the PCA analysis showed that the first two principal components of the

14　environmental factors accounted for 67% of the total variance of the normalised

15　environmental data. Co-variability between environmental factors is relatively high

16　because the explained variance is higher than the minimum value of the variance

17　explained by the first two PCs in the event all 9 factors were uncorrelated (i.e. [2/9]= 22

18　%). Most variance in the environmental data set was found in SST, Si and NO_{2+3}

19　concentrations. In late winter, low temperatures and salinity co-occurred with relatively

20　turbid and NO_{2+3} -rich waters. From spring until the start of summer, high chlorophyll-

21　concentrations co-occurred with low phosphate and ammonium concentrations,

22　followed by the highest values of daily insolation, which coincided with low silicate

23　concentrations. The highest water temperatures were found at the end of summer,

24　which co-occurred with the highest salinities and relatively clear and NO_{2+3} -poor

1   waters. Finally, from early to mid-winter low chlorophyll-concentrations were found

2   which co-occurred with high phosphate and ammonium concentrations, followed by the

3   lowest values of daily insolation, which coincided with high silicate concentrations.

4   *3.2 Production-light (PE) curves*

5   For the years 2012, 2013 and 2014, in total 107 incubations were performed. For these

6   days, production-light (PE) curves were fitted, using four models (Table 1, Figure 6): EP,

7   JP, PGH and Webb. The results of curve fits were compared between models using the

8   ssr and AIC criterion. Both the distribution of ssr and AIC scores are quite similar for the

9   four models but model 'Webb' had the highest ssr for all curve fits. A closer look at the

10   differences in ssr between models revealed that especially at small values for ssr (<20)

11   the models Webb, EP and PGH have a systematically higher ssr compared to model JP. In

12   addition, for each PE-curve fit it was determined which model had the lowest ssr, the

13   highest ssr and the lowest AIC score (Table 2), based on these counts it was decided that

14   the model JP was the best model for this dataset, with the lowest ssr and AIC for most

15   fits (51 and 75 out of 107 respectively).

16   Photosynthetic parameter estimates α^B and P^B_{max} were compared between models

17   (Table 3). With model PGH, α^B could not be estimated for two incubations and P^B_{max}

18   could not be estimated on 16 occasions. Depending on the model choice, the average

19   estimate for α^B is 28 % higher with model Webb, and 19% for PGH and EP compared to

20   the JP model. For P^B_{max} estimates, both model EP and PGH give estimates that are on

21   average 2 % higher compared to model JP, for model Webb this is on average 5 %.

22   Models EP and PGH allow for a fit including photo-inhibition, the estimates of β^B as

23   defined in this study (Material & Methods section) for both models gave a good

24   correlation (r = 0.94). For PGH, β^B could be estimated for 90 incubations, for EP this was

1   106 times. The estimated β^B from model PGH was on average 10 % lower compared to

2   the estimated β^B from model EP. The average estimate of β^B for model EP was 0.0015 ±

3   0.0015 mg C (mg Chl)$^{-1}$ h^{-1} (μmol photons m^{-2} s^{-1})$^{-1}$.

4   *3.3 Temporal variation in photosynthetic parameters*

5   To investigate the seasonal and year-to-year variation in photosynthetic parameters,

6   the results from model JP were used. Both α and P_{max} were normalised to chlorophyll-a

7   biomass (α^B and P^B_{max}). Values ranged between 0.00024 and 0.24 mg C (mg Chl)$^{-1}$ h^{-1}

8   (μmol m^{-2} s^{-1})$^{-1}$ for α^B with median values of 0.038, 0.019 and 0.016 in 2012, 2013 and

9   2014 respectively (Figure 7). Values for α^B were always higher in 2012 compared to the

10   values in 2013 and 2014, except for 1 outlier in 2013. Values showed little variation in

11   2014, in this year also the lowest absolute estimates for α^B were found (Figure 7 & 8).

12   P^B_{max} estimates varied between 0.1 and 48.9 mg C (mg Chl)$^{-1}$ h^{-1} with median values of

13   7.5, 4.6 and 5.2 for the three years (Figure 7). Both the absolute and the median

14   estimates for P^B_{max} were highest in 2012 compared to the two other years (Figure 7 &

15   8). In 2014, the lowest absolute values for P^B_{max} were found. Apart from the outliers,

16   there was a general increase in the value of P^B_{max} from the end of spring to the end of

17   September (day 270). In 2013, low values for the first months of the year (up until day

18   110, end of April) correspond to low water temperatures in the same period (Figure 4).

19   In 2012, there is a peak in the estimates for both α^B and P^B_{max} in October and November

20   (day 283 and 306) (Figure 7 & 8), which does not correspond to a high chlorophyll-a

21   concentration, nor to a high water temperature (Figure 4 & 5). The estimates for P^B_{max}

22   and α^B were highly correlated (Figure 9) and α^B can be estimated from P^B_{max} from the

23   linear relation α^B =0.05 ± 0.02 + 0.13 ± 0.01 $P^B_{max,}$ explaining 64% of the variance ($F_{1,105}$

24   = 188.4, p < 0.0001). The parameter E_k (μmol m^{-2} s^{-1}), calculated as P^B_{max}/ α^B, represents

1   the irradiance at which light becomes saturating. Throughout the year, estimates for Ek

2   were lowest for 2012. As for P^B_{max}, there was an increase from spring towards autumn

3   (Figure 7 & 8).

4   *3.4 The relation of photosynthetic parameters with environmental parameters*

5   For α^B, there was no significant univariate correlation with any of the environmental

6   variables (Figure 10). P^B_{max} correlated positively with sea surface temperature (SST)

7   and negatively with nitrite/nitrate (NO_{2+3}) silicate (Si) and the vertical light attenuation

8   coefficient (K_d) (Figure 10) when all years were analysed together. These variables

9   were included in multivariate linear models. Adding year as a factor to the models

10 always resulted in a lower AIC than similar models without the year effect (Supplement

11 2).

12 The best model, based on the lowest AIC, was a model that included year and sea

13 surface temperature. The difference in AIC of this model compared to that of next best is

14 2 (model 3b, Supplement 2), indicating that these two models are comparably good

15 (Burnham & Anderson 2004). In such a case, the simplest model should be considered.

16 As long as it remains unknown which environmental condition(s) determine(s) this

17 additional year-to-year variation, the best model that could provide satellite-derived

18 information for P^B_{max} is a model that included sea surface temperature only. A model

19 that included SST and a model that include both SST and Silicate (Supplement 2) could

20 equally well describe the variation in Ek.

21 *3.5 Daily and annual primary production*

22 Estimates for the daily column production, using model JP, ranged from to 3.4 mg to 3.8

23 g C m^{-2} per day, with large differences between the three years (Figure 11). The average

1 daily production was 0.54 g C m^{-2} d^{-1} in 2012, 0.65 g C m^{-2} d^{-1} in 2013 and 0.36 m^{-2} g C d^{-1}

2 in 2014. For 2012, 2013 and 2014, the annual production was 198, 239 and 131 g C m^{-2}

3 per year, respectively (Table 4). When the estimates of the yearly production based on

4 curve fits from model JP are compared with estimates based on the models EP, PGH or

5 Webb, the model JP gives the lowest estimates, except for one occasion (EP in 2013)

6 (Table 4). The annual production estimates from the three other models give an

7 estimate within 10 % deviation, except for the estimate for 2014 using model PGH, here

8 this models estimates are 17 % higher compared to model JP.

9 ## 4. Discussion

10

11 *4.1 Model choice*

12 Production-light curves were fitted, using four different models, being JP (Jassby & Platt

13 1976) and Webb (Webb et al. 1974) without a parameter for photo-inhibition and EP

14 (Eilers & Peeters 1988) and PGH (Platt, Gallegos & Harrison 1980) with a parameter for

15 photo-inhibition. The PGH model was unable to estimate P^B_{max} on 16 occasions, but in

16 the calculations of the annual production, the parameter P_s is used (Table 1); this

17 parameter was estimated for all incubations. Different models gave different estimates

18 for photosynthetic parameters as well as estimates of production (this paper), so it is

19 important to choose one model to analyse the data. In the current study, model JP was

20 selected as the best model to analyse the data, however, model JP is a model without a

21 photo-inhibition parameter, while it was seen that the carbon fixation rate is sometimes

22 lowered at the highest irradiances (e.g. 19 June 2012, Figure 6) suggesting the

23 occurrence of photo-inhibition. In the current study, algal cells in small bottles were

24 exposed to irradiances up to 1700 µmol photons m^{-2} s^{-1} for a period of two hours. Such

1   endured exposure to high light can result in more severe photo-inhibition compared to

2   phytoplankton cells in the water column, where water mixing reduces the time spent in

3   the euphotic zone (Peterson 1980, Grobbelaar 1985). The occasional depression of the

4   carbon fixation rate at high irradiances might thus be partly the result of an incubation

5   artefact.

6   How likely is a reduction of carbon fixation rates *in situ* due to exposure to excess

7   irradiance in the western Wadden Sea? According to MacIntyre et al. (2002), photo-

8   inhibition is most likely to occur in mixed shallow waters where the mean water column

9   irradiance is larger than the value for E_k. At the sampling location, the average column

10   irradiance (I_{av}, µmol photons m^{-2} s^{-1}) per day was calculated using the maximum surface

11   irradiance during a sampling day and the attenuation coefficient cf. MacIntyre & Cullen

12   (1996). Occasionally I_{av} was higher than E_k indicating that photo-inhibition can occur.

13   However, Grobbelaar (1985) argued that in mixed waters the severity of photo-

14   inhibition is minimised since algal cells move rapidly in and out the photic zone. In

15   turbid areas, the non-photic zone might be quite large. If the mixing depth is larger than

16   the euphotic zone, which is the case at the study location, algal cells likely spent more

17   time in the dark. Falkowski et al. (1993) recorded mid-day depressions in the

18   photosynthetic efficiency using fast repetition rate fluorescence (frrf) measurements

19   and the authors considered changes in the ratio of the variable fluorescence to

20   maximum fluorescence (F_v/F_m) to be a reliable means to identify the occurrence of

21   photo-inhibition in a system. At the Marsdiep jetty, short-term light curves based on frrf

22   measurements are applied since 2014 in addition to the ^{14}C incubations at the

23   laboratory. Data from these *in situ* measurements suggest that photo-inhibition does not

24   occur at this location (Kromkamp et al. in prep.). In addition, when considering the

1   differences in annual production estimated by the four models, it is seen that model JP

2   generally had the lowest annual production estimates compared to all other models

3   (Table 4). If photo-inhibition would have an effect on the production estimates, a model

4   without photo-inhibition would overestimate the production. Choosing a model without

5   a photo-inhibition term to analyse the data thus seem legitimate here.

6

7   *4.2 Photosynthetic parameters*

8   The estimates for the photosynthetic parameters from the JP model were compared to

9   the estimates from the other three models. The estimates for α^B from the other models

10   were between 13 and 28 % higher compared to the JP estimates, while for P^B_{max} the

11   estimates were more comparable between models with 1-5 % difference (Table 3). The

12   difference in estimates for α^B and P^B_{max} between models as well as the higher variability

13   in estimates for α^B have been reported before (e.g. Jassby & Platt 1976, Frenette et al.

14   1993, Kromkamp & Peene 1995). When comparing the JP model with the Webb model,

15   Frenette et al. (1993) concluded that the estimates for both parameters with the model

16   of Webb were higher that the estimates made with the model JP. Kromkamp & Peene

17   (1995) observed that the P^B_{max} obtained with the JP model was slightly smaller (< 10 %)

18   than when obtained with the EP method whereas the opposite was observed for α^B ($\sim$ 4

19   % higher).

20   Theoretical maxima for respectively α^B and P^B_{max} are defined as 0.11 mg C (mg Chl)$^{-1}$ h^{-1}

21   (μmol photons m^{-2} s^{-1})$^{-1}$ and 25 mg C (mg Chl)$^{-1}$ h^{-1} (Platt & Jassby 1976, Falkowski

22   1981, Lohrenz et al. 1994). In the current study, estimates for α^B were higher than this

23   maximum on two occasions (on day 132 in 2012 and day 115 in 2013), and for P^B_{max} on

24   three occasions (the same days as for α^B and on day 236 in 2012) (Figure 7 & 8). Visual

1   inspection of the curves did not reveal any abnormalities. Rates higher than the

2   theoretical maxima have been reported in other studies as well and were in those cases

3   related to low chlorophyll-a concentrations due to the dominance of small, but very

4   productive cells (Lohrenz et al. 1994, Azevedo et al. 2010). Low chlorophyll-a

5   concentrations could also be the result of mistakes during filtration or incomplete

6   extraction of pigments. In the current study the chlorophyll-a concentrations on the

7   dates with high values for the PE-parameters did not correspond to very low values of

8   chlorophyll-a, but the possibility that the concentrations were too low cannot be

9   excluded. When relating environmental variables to the PE-parameters, the removal of

10   outliers (see material and methods), which corresponded to the values higher than the

11   theoretical maxima, improved the predictive model for P^B_{max} (Supplement 2).

12   Bouman et al. (2018) reported minimum values for P^B_{max} to be 0.2 mg C (mg Chl) $^{-1}$ h^{-1}

13   and 0.002 mg C (mg Chl)$^{-1}$ h^{-1} (μmol photons m^{-2} s^{-1})$^{-1}$ for $α^B$. Values for $α^B$ and P^B_{max}

14   lower than these rates were recorded on 19 and 22 May 2014.

15   Apart from the extreme values for $α^B$ and P^B_{max}, the reported estimates for $α^B$ and P^B_{max}

16   in the current study were high compared to estimates reported in other studies. Within

17   the Wadden Sea area, Tillmann et al. (2000) reported for the southern part of the

18   German Wadden Sea that in 1995-1996, using the model of PGH, $α^B$ varied between

19   0.007 and 0.039 mg C (mg Chl)$^{-1}$ h^{-1} (μmol photons m^{-2} s^{-1})$^{-1}$ and for P^B_{max} between 0.8

20   and 9.9 mg C (mg Chl)$^{-1}$ h$^{-1.}$ In the current study, for 2012, the median values for $α^B$ and

21   P^B_{max} in 2012 were close to the maximum values reported in Tillmann et al. (2000). The

22   maximum value in the current study was almost twice the maximum recorded in that

23   study. Loebl et al. (2007) reported for the northern part of the German Wadden Sea in

24   2004 estimates between 0.014 and 0.13 mg C (mg Chl)$^{-1}$ h^{-1} (μmol photons m^{-2} s^{-1})$^{-1}$ for

1   α^B, between 1.8 and 14 mg C (mg Chl)$^{-1}$ h^{-1} for P$^B_{max}$, and between 107 and 360 μmol

2   photons m^{-2} s^{-1} for E$_k$. There, the PGH model was used for curve fitting. Closer to the

3   sampling location of the current study, Brinkman et al. (2015) reported that estimates

4   in 2012-2013 for several locations on a transect from the Dollard towards the North

5   Sea, ranged between 0.005 and 0.25 mg C (mg Chl)$^{-1}$ h^{-1} (μmol photons m^{-2} s^{-1})$^{-1}$ for α^B

6   and between 1 and 22 mg C (mg Chl)$^{-1}$ h^{-1} for P$^B_{max}$. Brinkman et al. (2015) used the EP

7   model for curve fitting. Kamermans et al. (2014) reported that for the Marsdiep area,

8   using model PGH, α^B ranged between 0.02 and 0.12 mg C (mg Chl)$^{-1}$ h^{-1} (μmol photons

9   m^{-2} s^{-1})$^{-1}$ in period 2011-2013, while values for P$^B_{max}$ were between 4 and 12 mg C (mg

10   Chl)$^{-1}$ h^{-1} (values were read from the graph). Kamermans et al. (2014) also recorded

11   photosynthetic parameter values for the same sampling location as the current study

12   (Jetty, but then at low tide) with α^B ranging between 0.01 and 0.1 mg C (mg Chl)$^{-1}$ h^{-1}

13   (μmol photons m^{-2} s^{-1})$^{-1}$ for 2011-2012 (April – October) and P$^B_{max}$ between 2 and 10

14   mg C (mg Chl)$^{-1}$ h^{-1}. The estimates for the photosynthetic parameter α^B in the current

15   study is comparable, while for P$^B_{max}$ the estimates are somewhat higher. The values for

16   E$_k$ ranged between 60 and 540 μmol photons m^{-2} s^{-1} (Figure 7 & 8), with minimum

17   values at the low end of what was recorded for E$_k$ according to Kirk (1994) (between

18   200-500 μmol photons m^{-2} s^{-1}), but comparable to values reported for other locations in

19   the Wadden Sea area (Tillmann et al. 2000, Loebl et al. 2007).

20   *4.3 Photosynthetic parameters related to environmental variables*

21   In the current study, the estimates for both α^B and P$^B_{max}$ varied throughout the year. The

22   values for α^B showed no correlation with any of the environmental variables considered

23   in this study, while for P$^B_{max}$ there were significant positive correlations with sea surface

24   temperature and salinity and negative correlations with the vertical light attenuation

1   coefficient, silicate and nitrite+nitrate concentration (Figure 10). Using (a combination

2   of) environmental variables to predict P^B_{max} resulted in a model that could explain a

3   maximum of 30% of the variation (Supplement 2). The best model, based on the lowest

4   AIC and highest R^2 was a model that included year, and SST, after removing the extreme

5   values, all other environmental variables did not contribute significantly to the

6   explained variance in P^B_{max} (Supplement 2). Since the variation in P^B_{max} due to the

7   factor year cannot be estimated based on remote sensing data, P^B_{max} can be described

8   by sea surface temperature, as 2.06 ± 0.67 + 0.30 ± 0.05 x SST, explaining 28% of the

9   variation. This percentage of explained variance is equal to the 28% reported in Platt &

10   Jassby (1976), but much lower than the 74-95 % explained variance by water

11   temperature as was reported in Rae & Vincent (1998). The latter study however was

12   performed under constant laboratory conditions using monocultures of phytoplankton

13   species. Many studies report an exponential relation between SST and P^B_{max} (e.g. Eppley

14   1972, Lohrenz et al. 1994, Tillmann et al. 2000, Macedo et al. 2001), but in the current

15   study a linear relation gave the best fit to the data. In 2012 values for P^B_{max} were higher

16   than in the other two years, while sea surface temperature was lower compared to 2014

17   for most of the year (Figure 4). The fact that SST was the variable that explained most of

18   the variation in values of P^B_{max} does not necessarily indicate that there is a direct effect

19   of temperature on this photosynthesis parameter since SST correlates with other

20   environmental variables including nutrient concentrations (this study) as well as

21   species composition (Richardson et al. 2016). However, as P^B_{max} is driven by the rate of

22   carbon fixation, the enzymatic processes in the carbon cycle, a direct effect of

23   temperature on P^B_{max} is to be expected and this has been demonstrated with culture

24   studies (e.g. Morris & Kromkamp 2003).

1   Previous studies have found mixed results with the variation in α^B both independent of

2   temperature (Post et al., 1985), as well as depended on water temperature (Lohrenz et

3   al., 1994). Estimates for α^B have also been correlated to irradiance (or average of

4   irradiance of three days previous) (Platt & Jassby 1976). For P^B_{max} variation was

5   explained by total irradiance and water temperature (Shaw & Purdie 2001, Rae &

6   Vincent 1998) or water temperature alone (Platt & Jassby 1976, Lohrenz et al. 1994).

7   A strong correlation between α^B and P^B_{max} was observed. A-priori such a relationship is

8   not to be expected as α^B is related to pigment composition and the chance to absorb a

9   photon, whereas P^B_{max} is related to processes downstream in photosystem II (PSII).

10   Classical photo-acclimation, i.e. by changing the absorption cross section of the antenna

11   by adding more or less photosynthetic pigments, will primarily affect α^B, but not

12   necessarily P^B_{max}. However, many studies (Behrenfeld et al. 2004, Bouman et al. 2018

13   and references in both papers) observed linear relationships between α^B and P^B_{max}, as in

14   the current study. This positive correlation has been attributed in a review by Bouman

15   et al. (2018) to "a variety of physiological and ecological factors, including changes in

16   the allocation of ATP and NADPH to carbon fixation (Behrenfeld et al., 2004), as well as

17   changes in phytoplankton community structure (Côté and Platt, 1983)".

18   From the abiotic variables that can be estimated at present from Earth Observation

19   data, P^B_{max} can be indirectly estimated from SST (and underwater light-climate)

20   (Behrenfeld & Falkowski 1997, Cox et al 2010), while α^B can be derived from P^B_{max}. The

21   low variability in α^B and P^B_{max} explained by environmental variables impedes the

22   estimation of primary production from remotely sensed data.

23   E_k is generally used as an indicator of the photo-acclimation state of the phytoplankton

24   community (Sakshaug et al. 1997). As was described by Sakshaug et al. (1997) "at lower

1   irradiances, the quantum yield of photosynthesis is higher, but the photosynthetic rate

2   is lower; at higher irradiances, there is no major increase in the photosynthetic rate and,

3   hence, nothing to be gained, and potentially much to be lost. Consequently, if the

4   irradiance increases, the algae adjust their E_k upwards and vice versa". Based on this

5   principle it was expected that variation in E_k could be related to surface irradiance (E_0),

6   the underwater light attenuation coefficient (K_d) or a product of both. In the current

7   study, E_k correlated significantly with e.g. SST and the underwater light attenuation, but

8   not with surface irradiance (Figure 10). A model with K_d (with and without E_0) only

9   explained 16% of the variation in E_k, while a model with SST explained 41%

10   (Supplement 2). The absence of a relation between E_k and (a product of) E_0 and K_d is

11   unexpected and there is no satisfactory explanation for this finding.

12   *4.4 Daily and annual primary production estimates*

13   In the current study, no attempts were made to estimate respiratory losses in the dark.

14   Autotrophic respiration under certain conditions might be large, resulting in a negative

15   net photic zone production. In turbid areas, the euphotic depth (Z_{eu}) might be smaller

16   than the mixing depth (Z_{mix}), exposing the phytoplankton community to light intensities

17   too low to support photosynthesis. To sustain positive net phytoplankton growth, the

18   ratio between the euphotic depth and the mixing depth (Z_{eu}: Z_{mix}) should be above 0.2

19   (e.g. Grobbelaar 1985, Cloern 1987, Alpine & Cloern 1988, Kromkamp & Peene 1995),

20   which was the case at the sampling location although the study by Kromkamp & Peene

21   also obtained evidence that it might be smaller than 0.2.

22   The daily water column production ranged from 3.4 to 3800 mg C m^{-2} d^{-1}. Whether ^{14}C

23   incubations best represent net of gross production rates is still under debate (Halsey et

24   al. 2010, 2013, Pei & Laws, 2013, Milligan et al. 2015). The rates of daily carbon fixation

1   as well as the annual production presented in this paper are therefore refer to as

2   'production rates'. The seasonal pattern in the daily production rates were comparable

3   with the pattern seen in chlorophyll-a concentrations as has been described in other

4   studies in the Wadden Sea (Tillmann et al. 2000). There were large differences in annual

5   production between the years with an annual production in 2013, which was 80 %

6   higher than the production in 2014, the year with the lowest annual production and 25

7   % higher than the production in 2012 (Table 4). This difference is largely due to the

8   difference in chlorophyll-a concentration in spring (Figure 5). Recent findings showed

9   that the timing of the spring bloom is initiated by underwater light climate, while the

10 build-up of zooplankton biomass is driven by water temperature (Wiltshire and

11 Boersma, 2016). One explanation for the higher chlorophyll-a concentration in spring in

12 2013, is that the low water temperature in the first half of the year (Figure 4)

13 suppressed zooplankton biomass, reducing grazing rates and thus allowing for a higher

14 achieved phytoplankton biomass. In addition, the higher concentrations of silicate in

15 2013 compared to both other years in the pre-bloom period might have resulted in a

16 higher phytoplankton biomass as this might delay the onset of Si-limitation for diatoms

17 (Ly et al 2014). In 2014, water temperatures were high year round, resulting in more

18 severe grazing, especially later in the season, explaining the low and late autumn peak

19 in chlorophyll-a this year (Figure 5).

20 Production rates for the same location as in the current paper have been published by

21 Cadée & Hegeman (1974, 2002) and more recently by Philippart et al. (2007). Both

22 papers present the results on carbon fixation rates using ^{14}C, but incubated samples at

23 one fixed light intensity only. In addition, Cadée & Hegeman did not consider the daily

24 irradiances when calculating daily production rates, and assumed that light conditions

1   were saturating during incubation. Therefore, the results from the current study will

2   only be compared with the results published by Philippart et al. (2007). Philippart et al.

3   (2007) followed a different procedure to calculate carbon-fixation rates, which resulted

4   in an 8% lower estimate of the daily column production compared to the current study

5   (Supplement 3). The annual production estimates for the period 1990-2004 lay

6   between 120 and 310 g C m^{-2} y^{-1} and showed a steady decline over this period

7   (Philippart et al. 2007). The annual primary production for 2012-2014 (this paper) is

8   comparable to that of the early 2000s reported by Philippart and co-authors (2007). It

9   thus seems that the decline in primary production, noted by Philippart et al., has come

10 to a halt (or even slightly reversed) (Figure 12). The decline in production in the

11 western Wadden Sea was the result of reduced riverine nutrient inputs since the mid-

12 1980s. Since the 2000s the decline in phosphate load has nearly come to a halt and P-

13 concentrations are now comparable to the concentrations before the 1970-ies, while N-

14 loads have been reduced to a lower extent (Cadée & Hegeman, 2002, Supplement 4).

15 It is assumed that primary production in the western Wadden Sea in spring is P-limited

16 with likely P-Si-co-limitation for diatoms (Ly et al. 2014). Along the Dutch coast long-

17 term nutrient concentrations show a similar pattern as in the western Wadden Sea

18 (Supplement 4), suggesting that the rate of pelagic primary production might also have

19 decreased and have come to a halt here, and potentially also in other coastal seas in

20 Europe. Additional analysis is needed to see whether the decrease in annual primary

21 production is confined to the western part of the Wadden Sea or that the low

22 production rates are found throughout the whole Wadden Sea. Continuation of

23 monitoring primary production is essential to find out whether the decline had halted

24 or whether it will continue to decline in the future.

1   ## 5. Conclusions

2

3   The equation from Jassby & Platt (1976) was selected as the best model to analyse

4   production-irradiance data in the current study. This JP model is a model without a

5   parameter that allows for a reduction on the carbon fixation rate at high irradiances.

6   Estimates for α^B varied between 0.00024 and 0.24 mg C (mg Chl)$^{-1}$ h^{-1} (µmol m^{-2} s^{-1})$^{-1}$

7   and for P^B_{max} between 0.1 and 48.9 mg C (mg Chl)$^{-1}$ h^{-1}. The estimates for α^B and P^B_{max}

8   were correlated and showed seasonal variation with, on average, higher values in

9   summer and peaks in spring. There were considerable differences in values for

10   photosynthetic parameters between years, with the highest estimates in 2012 (150%

11   higher than in 2013, 300% higher than in 2014). The best model to estimate P^B_{max} was a

12   model that included SST and year, but the underlying causes of this 'year-effect' remain

13   unsolved for now. With respect to available information in space and time from Earth

14   Observations, P^B_{max} can thus be derived from SST, explaining 28% of the variance. The

15   absence of a correlation between α^B and environmental variables, the relatively large

16   unresolved variance in the estimates for P^B_{max} and the large differences between years

17   indicate that there still is some way to go before satellite measurements can be used for

18   monitoring temporal and spatial variation in productivity.

19   Daily primary production varied between years with an average of 0.54 g C d^{-1} in 2012,

20   0.65 g C d^{-1} in 2013 and 0.36 g C d^{-1} in 2014. Annual production was calculated by linear

21   interpolation of all parameters except irradiance, which was available for all days. The

22   interpolated annual production for each of the three years was always lowest when

23   using the PE- curve fit from Jassby & Platt (1976), but differences between models were

24   relatively small (less than 10 %) between the lowest and highest estimate. Comparing

1 the estimates for the years 2012, 2013 and 2014 with estimates published earlier

2 indicated that the decline in planktonic primary production in the Marsdiep area since

3 the 1990s has come to a halt. Further research will be needed to investigate the possible

4 mechanisms underlying these changes.

5

6 Acknowledgements

7

19

20

1 Literature

2

3 Alpine, AE, Cloern, JE (1988). Phytoplankton growth rates in a light-limited

4 environment, San Francisco Bay. Mar Ecol Prog Ser 44:167-173.

5 Arbones, B, Figueiras, FG, Varela, R (2000). Action spectrum and maximum quantum

6 yield of carbon fixation in natural phytoplankton populations: implications for primary

7 production estimates in the ocean. J Mar Syst 26:97-114.

8 Aurin, DA, Dierssen, HM (2012). Advantages and limitations of ocean color remote

9 sensing in CDOM-dominated, mineral-rich coastal and estuarine waters. Remote Sens

10 Environ 125:181-197.

11 Azevedo, IC, Duarte, P, Bordalo, AA (2010). Temporal and spatial variability of

12 phytoplankton photosynthetic characteristics in a southern European estuary (Douro,

13 Portugal). Mar Ecol Prog Ser 412: 29-44.

14 Behrenfeld, MJ, Falkowski, PG (1997). A consumer's guide to phytoplankton primary

15 productivity models. Limnol Oceanogr 42:1479-1491.

16 Bouman, HA, Platt, T, Doblin, M, Figueiras, FG, Gudmundsson, K, Gudfinnsson, HG,

17 Huang, B, Hickman, A, Hiscock, M, Jackson, T, Lutz, VA, Mélin, F, Rey, F, Pepin, P, Segura,

18 V, Tilstone, GH, Dongen-Vogels, van V, Sathyendranath, S (2018). Photosynthesis–

19 irradiance parameters of marine phytoplankton: synthesis of a global data set. Earth

20 Syst Sci Data 10:251-266.

21 Brinkman, AG, Riegman, R, Jacobs, P, Kühn, S, Meijboom, A (2015). Ems-

22 Dollard primary production research, full data report. IMARES report C160/14, IMARES

23 Wageningen UR, Den Burg, Texel, the Netherlands, 297 pp.

1   Burnham, KP, Anderson, DR (2004). Multimodel inference: understanding AIC and BIC

2   in model selection. Sociol Method Res 33: 261-304.

3   Cadée, GC, Hegeman, J (1974). Primary production of the benthic microflora living on

4   tidal flats in the Dutch Wadden Sea. Neth J Sea Res 8:240-259.

5   Cadée GC, Hegeman, J (2002). Phytoplankton in the Marsdiep at the end of the 20th

6   century; 30 years monitoring biomass, primary production, and *Phaeocystis* blooms. J

7   Sea Res 48:97-110.

8   Chen, J, Zhang, M, Cui, T, Wen, Z (2013). A review of some important technical problems

9   in respect of satellite remote sensing of chlorophyll-a concentration in coastal waters.

10   IEEE J Sel Top Appl 6: 2275-2289.

11   Cloern, JE (1987). Turbidity as a control on phytoplankton biomass and productivity in

12   estuaries. Cont Shelf Res 7:1367-1381.

13   Cloern, JE (1999). The relative importance of light and nutrient limitation of

14   phytoplankton growth: a simple index of coastal ecosystem sensitivity to nutrient

15   enrichment. Aquat Ecol 33:3-15.

16   Cole, BE, Cloern, JE (1984). Significance of biomass and light availability to

17   phytoplankton productivity in San Francisco Bay. Mar Ecol Prog Ser 17:15-24.

18   Cole, BE, Cloern, JE (1987). An empirical model for estimating phytoplankton

19   productivity in estuaries. Mar Ecol Prog Ser 36:299-305.

20   Côté, B, Platt, T (1983). Day-to-day variations in the spring-summer photosynthetic

21   parameters of coastal marine phytoplankton. Limnol Oceanogr 28:320-344.

1 Cox, TJS, Soetaert, K, Vanderborght, JP, Kromkamp, JC, Meire, P (2010). Modeling

2 photosynthesis-irradiance curves: Effects of temperature, dissolved silica depletion, and

3 changing community assemblage on community photosynthesis. Limnol Oceanogr

4 Methods 8:424-440.

5 Eilers, PHC, Peeters, JCH (1988). A model for the relationship between light intensity

6 and the rate of photosynthesis in phytoplankton. Ecol Modell 42:199–215.

7 Ekholm, P (2008). N: P ratios in estimating nutrient limitation in aquatic systems.

8 Finnish Environment Institute: 11-14.

9 Eppley, RW (1972). Temperature and phytoplankton growth in the sea. Fish. Bull 70:

10 1063-1085.

11 Evans, N, Games, DE, Jackson, AH, Matlin, SA (1975). Applications of high-pressure

12 liquid chromatography and field desorption mass spectrometry in studies of natural

13 porphyrins and chlorophyll derivatives. J Chromatogr A 115: 325-333.

14 Falkowski, PG, Raven, JA (2007). Aquatic Photosynthesis. Princeton University Press,

15 Princeton, 375 pp.

16 Falkowski, PG (1981). Light-shade adaptation and assimilation numbers. J Plankton Res

17 3:203-216.

18 Falkowski, PG, Greene, R, Kolber, Z (1993). Light utilization and photoinhibition of

19 photosynthesis in marine phytoplankton (No. BNL-49821; CONF-9309312-1).

20 Brookhaven National Lab., Upton, NY (United States).

21 Frenette, JJ, Demers, S, Legendre, L, Dodson, J (1993). Lack of agreement among models

22 for estimating the photosynthetic parameters. Limnol Oceanogr 38:679-687.

1 Gabarró, C, Font, J, Camps, A, Vall-llossera, M, Julià, A (2004). A new empirical model of

2 sea surface microwave emissivity for salinity remote sensing. Geophys Res Lett 31.1.

3 Grobbelaar, JU (1985). Phytoplankton productivity in turbid waters. J Plankton Res

4 7:653-663.

5 Halsey, KH, Milligan, AJ, Behrenfeld, MJ (2010). Physiological optimization underlies

6 growth rate-independent chlorophyll-specific gross and net primary production.

7 Photosynth Res 103:125-137.

8 Halsey, KH, O'Malley, RT, Graff, JR, Milligan, AJ, Behrenfeld, MJ (2013). A common

9 partitioning strategy for photosynthetic products in evolutionarily distinct

10 phytoplankton species. New Phytologist 198, 1030-1038.

11 Heip, CHR, Goosen, NK, Herman, PMJ, Kromkamp, J, Middelburg, JJ, Soetaert, K (1995).

12 Production and consumption of biological particles in temperate tidal estuaries.

13 Oceanogr Mar Biol Annu Rev 33:1-149.

14 Herlory, O, Richard, P, Blanchard, G (2007). Methodology of light response curves:

15 application of chlorophyll fluorescence to microphytobenthic biofilms. Mar Biol 153:91-

16 101.

17 Højerslev, NK (1978). Daylight measurements appropriate for photosynthetic studies in

18 natural sea waters. ICES J Mar Sci 38:131-146.

19 Holmes, RW (1970). The Secchi disk in turbid coastal waters 1. Limnol Oceanogr15:

20 688-694.

1 Jamet, C, Loisel, H, Kuchinke, CP, Ruddick, K, Zibordi, G, Feng, H (2011). Comparison of

2 three SeaWiFS atmospheric correction algorithms for turbid waters using AERONET-OC

3 measurements. Remote Sens Environ 115:1955-1965.

4 Jassby, AD, Platt, T (1976). Mathematical formulation of the relationship between

5 photosynthesis and light for phytoplankton. Limnol Oceanogr 21:540–547.

6 Joint, I, Groom, SB (2000). Estimation of phytoplankton production from space: current

7 status and future potential of satellite remote sensing. J Exp Mar Biol Ecol 250:233-255.

8 Kamermans, P, Jak, R, Jacobs, P, Riegman, R (2014). Groei en begrazing van mosselzaad,

9 primaire productie en picoplankton in de Waddenzee Technisch Rapport project.

10 Meerjarige effect- en productiemetingen aan MZI's in de Westelijke Waddenzee,

11 Oosterschelde en Voordelta. IMARES report C187/13, IMARES Wageningen UR,

12 Yerseke, the Netherlands, 46 pp.

13 Kirk, JTO (1994). Light and Photosynthesis in Aquatic Ecosystems. Cambridge

14 University Press, Cambridge.

15 Klemas, V (2011). Remote sensing of sea surface salinity: an overview with case studies.

16 J Coast Res 27:830-838.

17 Kromkamp, J, Peene, J (1995). Possibility of net phytoplankton primary production in

18 the turbid Schelde Estuary (SW Netherlands). Mar Ecol Prog Ser 121:249-259.

19 Lee, Z, Shang, S, Du, K, Wei, J (2018). Resolving the long-standing puzzles about the

20 observed Secchi depth relationships. Limnol Oceanogr 63:2321-2336.

1 Lewis, MR, Smith, JC (1983). A small volume, short-incubation-time method for

2 measurement of photosynthesis as a function of incident irradiance. Mar Ecol Prog Ser

3 13:99-102.

4 Loebl, M, Dolch, T, van Beusekom, JE (2007). Annual dynamics of pelagic primary

5 production and respiration in a shallow coastal basin. J Sea Res 58:269-282.

6 Lohrenz, SE, Fahnenstiel, GL, Redalje, DG (1994). Spatial and temporal variations of

7 photosynthetic parameters in relation to environmental conditions in coastal waters of

8 the northern Gulf of Mexico. Estuaries 17:779-795.

9 Longhurst, A, Sathyendranath, S, Platt, T, Caverhill, C (1995). An estimate of global

10 primary production in the ocean from satellite radiometer data. J Plankton Res 17:

11 1245-1271.

12 Ly, J, Philippart, CJM, Kromkamp, JC (2014). Phosphorus limitation during a

13 phytoplankton spring bloom in the western Dutch Wadden Sea. J Sea Res 88:109-120.

14 Macedo, MF, Duarte, P, Mendes, P, Ferreira, JG (2001). Annual variation of

15 environmental variables, phytoplankton species composition and photosynthetic

16 parameters in a coastal lagoon. J Plankton Res 23:719-732.

17 Macedo, MF, Ferreira, JG, Duarte, P (1998). Dynamic behaviour of photosynthesis-

18 irradiance curves determined from oxygen production during variable incubation

19 periods. Mar Ecol Prog Ser 165:31-43.

20 MacIntyre, HL, Cullen, JJ (1996). Primary production by suspended and benthic

21 microalgae in a turbid estuary: time-scales of variability in San Antonio Bay, Texas. Mar

22 Ecol Prog Ser 145:245-268.

1 MacIntyre, HL, Kana, TM, Anning, T, Geider, RJ (2002). Photoacclimation of

2 photosynthesis irradiance response curves and photosynthetic pigments in microalgae

3 and cyanobacteria 1. J Phycol 38:17-38.

4 Milligan, AJ, Halsey, KH, Behrenfeld, MJ (2015). Advancing interpretations of C-14-

5 uptake measurements in the context of phytoplankton physiology and ecology. J

6 Plankton Res 37: 692-698.

7 Morris, EP, Kromkamp, JC (2003). Influence of temperature on the relationship between

8 oxygen-and fluorescence-based estimates of photosynthetic parameters in a marine

9 benthic diatom (*Cylindrotheca closterium*). Eur J Phycol 38: 133-142.

10 Muller-Karger, FE, Miloslavich, P, Bax, NJ, Simmons, S, Costello, MJ, Sousa Pinto, I, ... &

11 Best, BD (2018). Advancing marine biological observations and data requirements of

12 the complementary essential ocean variables (EOVs) and essential biodiversity

13 variables (EBVs) frameworks. Front Mar Sci 5:211.

14 Nauw, JJ, Merckelbach, LM, Ridderinkhof, H, & Van Aken, HM (2014). Long-term ferry-

15 based observations of the suspended sediment fluxes through the Marsdiep inlet using

16 acoustic Doppler current profilers. J Sea Res 87: 17-29.

17 Pei, S. & Laws, EA (2013). Does the 14C method estimate net photosynthesis?

18 Implications from batch and continuous culture studies of marine phytoplankton. Deep-

19 Sea Res Pt I 82: 1-9.

20 Pennock, JR, Sharp, JH (1994). Temporal alternation between light-and nutrient

21 limitation of phytoplankton production in a coastal plain estuary. Mar Ecol Prog Ser 25:

22 275-288.

Pereira, HM, Ferrier, S, Walters, M, Geller, GN, Jongman, RHG, Scholes, RJ, ... & Coops, NC (2013). Essential biodiversity variables. Science 339:277-278.

Peterson, BJ (1980). Aquatic primary productivity and the 14C-CO2 method: a history of the productivity problem. Annu Rev Ecol Syst 11:359-385.

Philippart, CJ, Cadée, GC, van Raaphorst, W, Riegman, R (2000). Long-term phytoplankton-nutrient interactions in a shallow coastal sea: Algal community structure, nutrient budgets, and denitrification potential. Limnol Oceanogr 45: 131-144.

Philippart, CJM, Beukema, JJ, Cadée, GC, Dekker, R, Goedhart, PW, van Iperen, JM, Leopold, MF, Herman, PM (2007). Impacts of nutrient reduction on coastal communities. Ecosystems 10:96-119.

Platt, T, Jassby, AD (1976). The relationship between photosynthesis and light for natural assemblages of coastal marine phytoplankton 1. J Phycol 12:421-430.

Platt, T, Gallegos, CL, Harrison, WG (1980). Photoinhibition and photosynthesis in natural assemblages of marine phytoplankton. J Mar Res 38:687–701.

R Core Team (2018). R: A language and environment for statistical computing. R Foundation for Statistical Computing, Vienna, Austria, version 3.5.1 https://www.R-project.org/

Rae, R, Vincent, WF (1998). Phytoplankton production in subarctic lake and river ecosystems: development of a photosynthesis-temperature-irradiance model. J Plankton Res 20:1293-1312.

Redfield, AC (1958). The biological control of chemical factors in the environment. Am Sci 46:205–221.

1   Richardson, K, Bendtsen, J, Kragh, T, Mousing, EA (2016). Constraining the distribution

2   of photosynthetic parameters in the Global Ocean. Front Mar Sci 3:269.

3   Ridderinkhof, H (1988). Tidal and residual flows in the Western Dutch Wadden Sea II:

4   an analytical model to study the constant flow between connected tidal basins. Neth J

5   Sea Res 22:185-198.

6   Sakshaug, E, Bricaud, A, Dandonneau, Y, Falkowski, PG, Kiefer, DA, Legendre, L, Morel, A,

7   Parslow, J, Takahashi, M (1997). Parameters of photosynthesis: definitions, theory and

8   interpretation of results. J Plankton Res 19:1637-1670.

9   Shaw, PJ, Purdie, DA (2001). Phytoplankton photosynthesis-irradiance parameters in

10 the near-shore UK coastal waters of the North Sea: temporal variation and

11 environmental control. Mar Ecol Prog Ser 216:83-94.

12 Silsbe, GM, Malkin, SY (2015). Phytotools: Phytoplankton production tools. R package

13 Version 1.0. Available from https://CRAN.R-project.org/package=phytotools

14 Spiess, AN, Neumeyer, N (2010). An evaluation of R^2 as an inadequate measure for

15 nonlinear models in pharmacological and biochemical research: a Monte Carlo

16 approach. BMC Pharmacol 10:6.

17 Strickland, JD, Parsons, TR (1972). A practical handbook of seawater analysis. Bull Fish

18 Res Bd Can 167:311.

19 Talling, JF (1957). Photosynthetic characteristics of some freshwater plankton diatoms

20 in relation to underwater radiation. New Phytologist 56:29-50.

21 Tillmann, U, Hesse, KJ, Colijn, F (2000). Planktonic primary production in the German

22 Wadden Sea. J Plankton Res 22:1253-1276.

1   Webb, WL, Newton, M, Starr, D (1974). Carbon dioxide exchange of *Alnus rubra*: A

2   mathematical model. Oecologia 17:281–291.

3   Wiltshire, KH, Boersma, M (2016). Meeting in the middle: On the interactions between

4   microalgae and their predators or zooplankton and their food. In: Glibert, PM, Kana, TM

5   (eds.) Aquatic Microbial Ecology and Biogeochemistry: A Dual Perspective (pp215-223).

6   Springer, Cham.

1 *Table 1. Four models to fit the relationship between carbon fixation rates (P; mg C L^{-1} h^{-1}))*

2 *and irradiance (E; µmol photons m^{-2} s^{-1}). Equations and derived parameters were taken*

3 *from the original papers as well as from Arbones et al. (2000), Macedo et al. (1998) and*

4 *Frenette et al. (1993).*

Model	Nr of Parameters	Reference	Original equation	Derived parameters
EP	3	Eilers & Peeters (1988)	$P = \dfrac{E}{aE^2 + bE + c}$	$\alpha = \dfrac{1}{c}$, $P_{max} = \dfrac{1}{b+2\sqrt{ac}}$
		Herlory et al. (2007)	$P = \dfrac{E}{\dfrac{E^2}{\alpha E_k^2} + \dfrac{E}{P_{max}} - \dfrac{2E}{\alpha E_k} + \dfrac{1}{\alpha}}$	
JP	2	Jassby & Platt (1976)	$P = P_{max}\, tanh\left(\dfrac{\alpha\, E}{P_{max}}\right)$	
PGH	3	Platt, Gallegos & Harrison (1980)	$P = P_s\left[1 - exp\left(\dfrac{-\alpha E}{P_{max}}\right)\right] exp\left(\dfrac{-\beta E}{P_s}\right)$	$P_{max} = P_s\left[\dfrac{\alpha}{\alpha+\beta}\right]\left[\dfrac{\beta}{\alpha+\beta}\right]^{\beta/\alpha}$
Webb	2	Webb et al. (1974)	$P = P_{max}\left[1 - exp\left(\dfrac{-\alpha\, E}{P_{max}}\right)\right]$	

5

6

1   *Table 2. The squared sum of the residuals (ssr) of the PE- curve fit for the different models.*

2   *The number of incubations in the period 2012-2014 was 107, per model the number of*

3   *times this model had the lowest ssr and the number of times the model fit yielded the*

4   *highest ssr is given. The percentage of the times a model had the lowest AIC criterion is*

5   *also given.*

Model	Smallest ssr	Highest ssr	% lowest AIC
EP	35	28	8
JP	51	10	75
Webb	3	60	14
PGH	18	9	3

6

7

8   *Table 3. Estimates for α^B and P^B_{max} relative to the estimate from model fit according to:*

9   *JP=a X+ b, where X is either α^B and P^B_{max} from the models EP, PGH or Webb. For both the*

10   *intercept (b) and regression coefficient (a), the average value ± standard deviation is given*

11   *as well as the p-value ("ns" for values not significant, p > 0.05). The explained variance of*

12   *the regression is given as R^2.*

		a	p-value	b	p-value	R^2
α^B	EP	1.19±0.05	<0.0001	0.0022±0.0020	ns	0.853
	Webb	1.28±0.01	<0.0001	0.0005±0.0003	ns	0.996
	PGH	1.19±0.01	<0.0001	0.0009±0.0006	ns	0.984
P^B_{max}	EP	1.02±0.01	<0.0001	0.17±0.05	0.0003	0.996
	Webb	1.05±0.01	<0.0001	-0.09±0.04	0.04	0.998
	PGH	1.02±0.00	<0.0001	0.03±0.03	ns	0.999

13

14

1 *Table 4. The estimates of annual production (g C m^{-2} year^{-1}) and the average daily*

2 *production (g C m^{-2} d^{-1}) at the sampling location using curve fit parameters from the*

3 *different models.*

	2012		2013		2014	
model	annual PP	daily PP	annual PP	daily PP	annual PP	daily PP
JP	198	0.54 ± 0.51	239	0.65 ± 1.01	131	0.36 ± 0.36
EP	203	0.56 ± 0.52	236	0.65 ± 0.96	133	0.37 ± 0.36
PGH	214	0.59 ± 0.50	244	0.67 ± 1.04	153	0.42 ± 0.43
Webb	206	0.56 ± 0.53	249	0.68 ± 1.05	138	0.38 ± 0.38

4
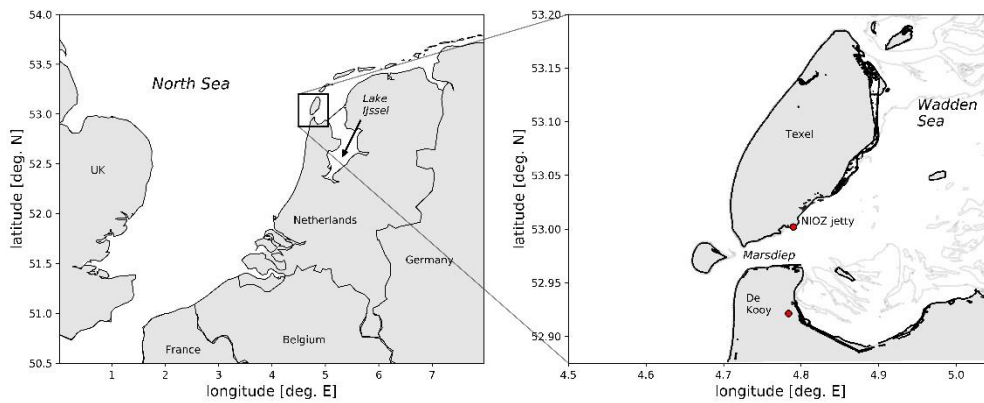
5

6 *Figure 1. Map of the study area, including the locations of the NIOZ Jetty sampling station,*

7 *the Marsdiep tidal inlet, the KNMI weather station "De Kooy" and the artificial freshwater*

8 *Lake IJssel. The grey lines in the right figure indicate the 1m depth contour.*

9
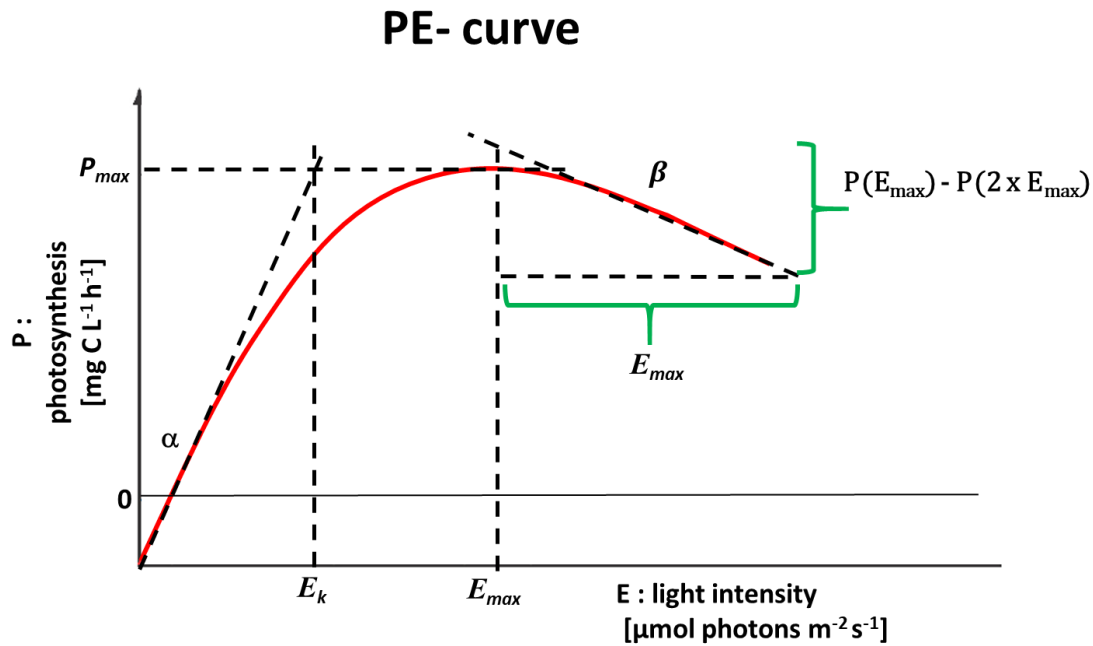
1

2 *Figure 2: Conceptual PE- curve, with the various parameters that define the*

3 *photosynthetic response of the sample's phytoplankton to increasing light intensities. Here*

4 *photo-inhibition is defined as $\beta = P(E_{max})-P(2 \times E_{max}))/E_{max}$ to allow for a comparison of*

5 *possible photo-inhibition between models. Note that β is defined as a positive, downward,*

6 *slope, to allow for comparison with other photo inhibition parameters. The light*

7 *saturation coefficient E_K can be calculated as P_{max}/α.*

8

9

A

B

1
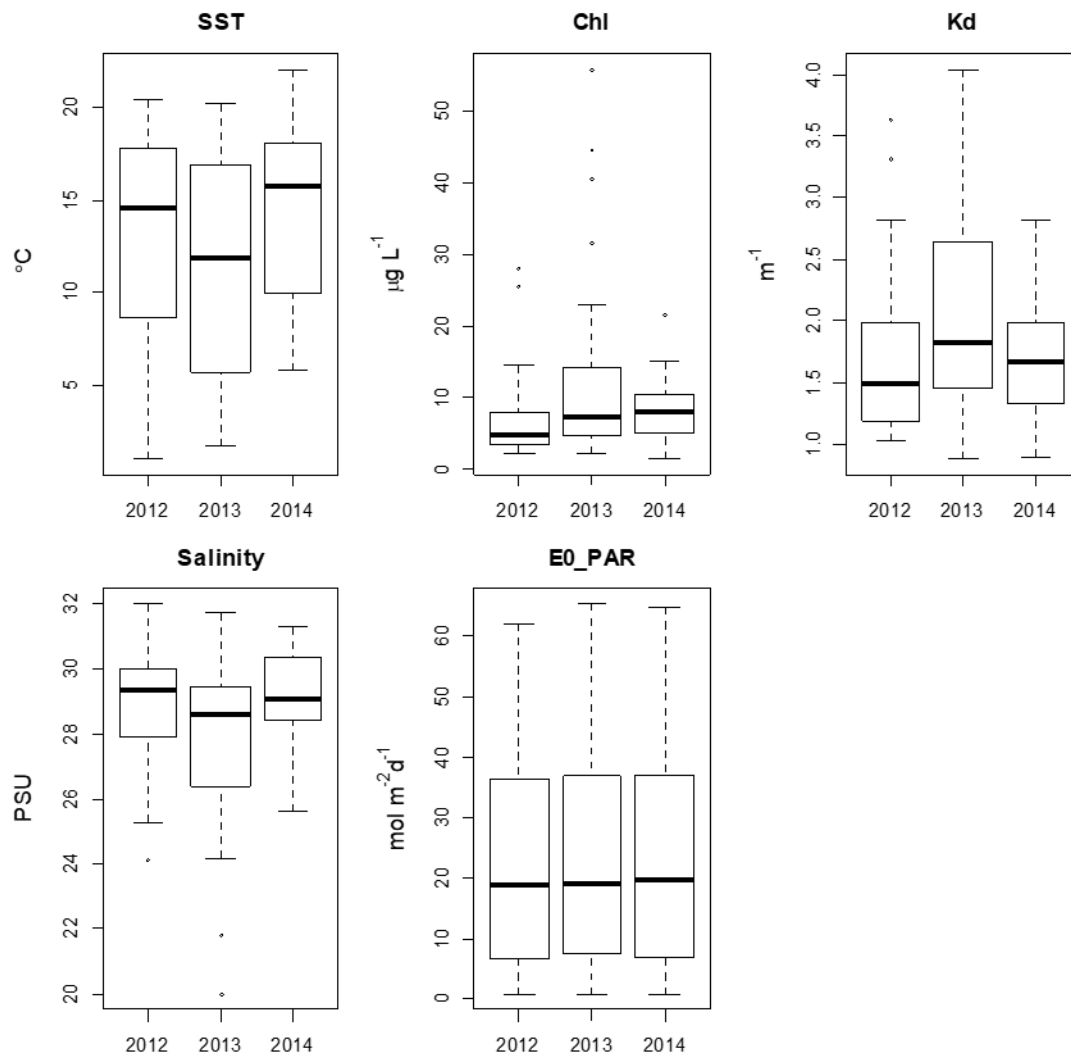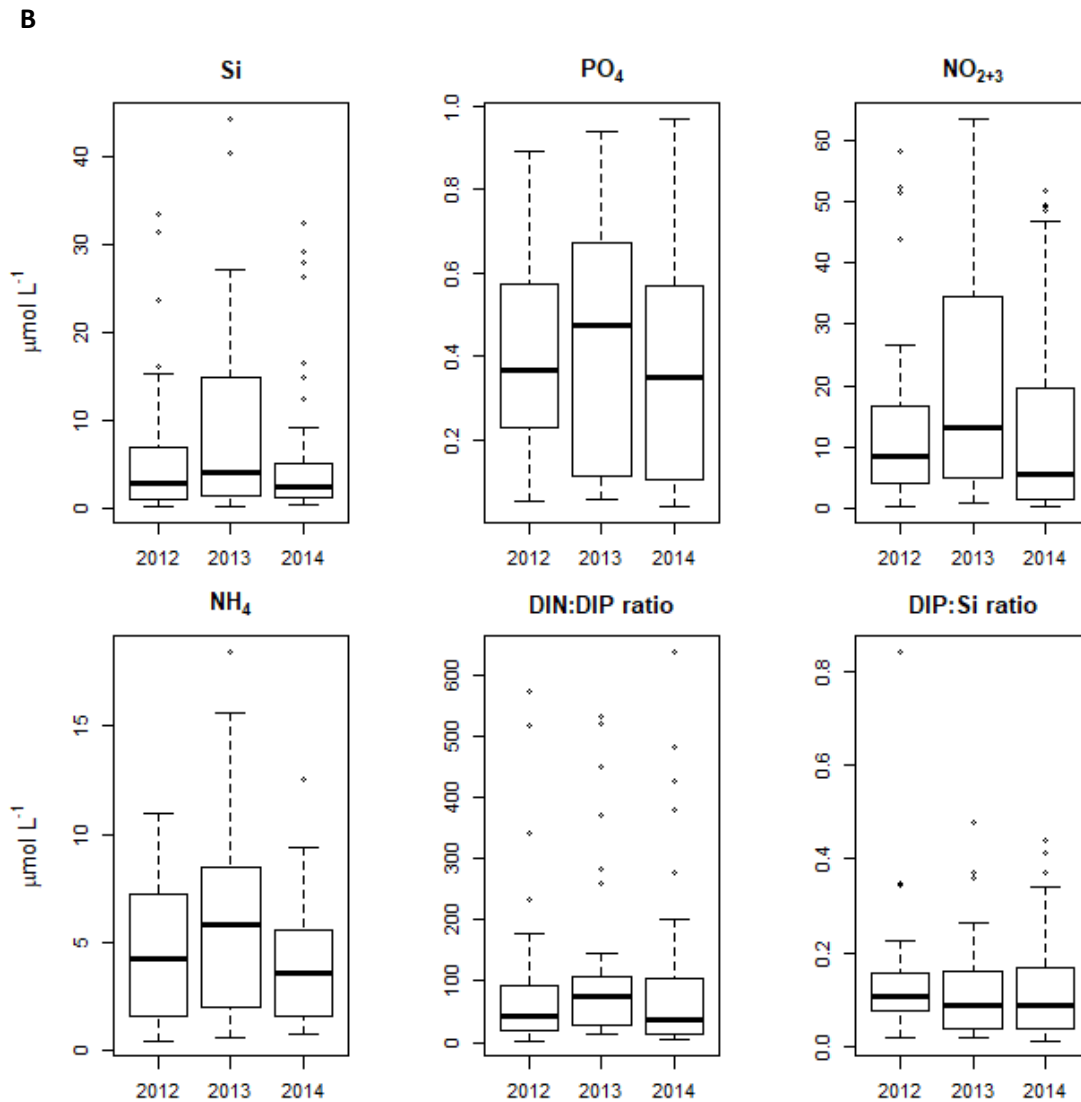
Figure 3. Box-whisker plots showing the median and interquartile range, minimum and

maximum values as well as outliers for the sampling dates, except for the daily sum of

irradiance, which is a mean for all days of the year. A: sea surface temperature (SST; °C),

phytoplankton biomass (Chl; µg L⁻¹), light attenuation coefficient (K_d; m⁻¹), salinity (PSU)

and the daily sum of surface irradiance (E_{PAR+0}; mol photons m⁻² d⁻¹) for the years 2012,

2013 and 2014. B: nutrient concentrations (µmol L⁻¹); silicate (Si), phosphate (PO₄), nitrite

+ nitrate (NO_{2+3}) and ammonium (NH₄), DIN:DIP ratio and DIP:Si ratio.

1
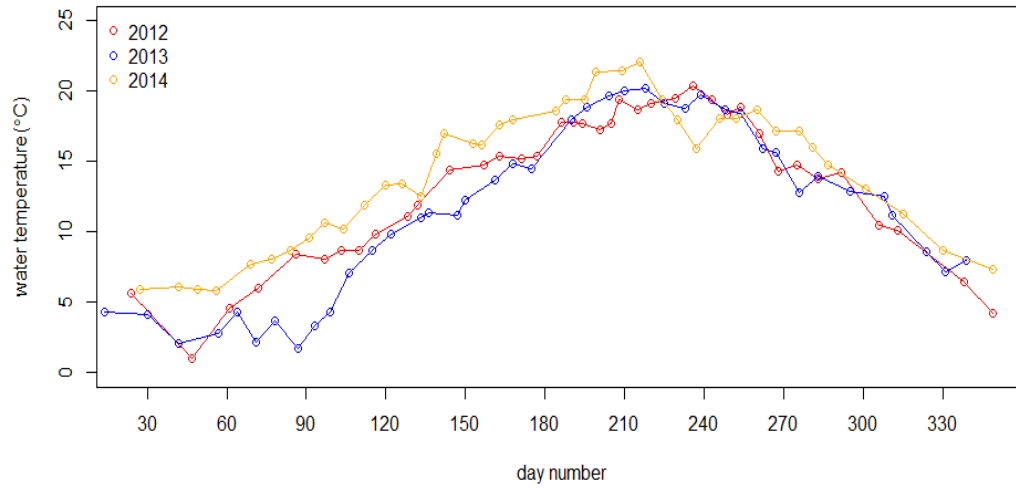
Figure 4. Sea surface temperature (SST; °C) at the Marsdiep jetty in the years 2012, 2013

and 2014.

4
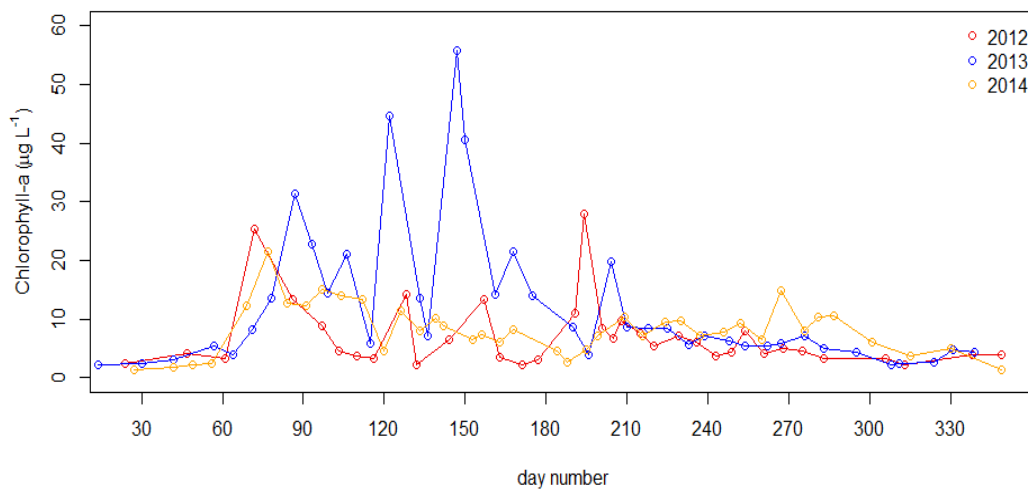
Figure 5. The chlorophyll-a concentration (µg L^{-1}) at the Marsdiep jetty in the years 2012,

2013 and 2014.
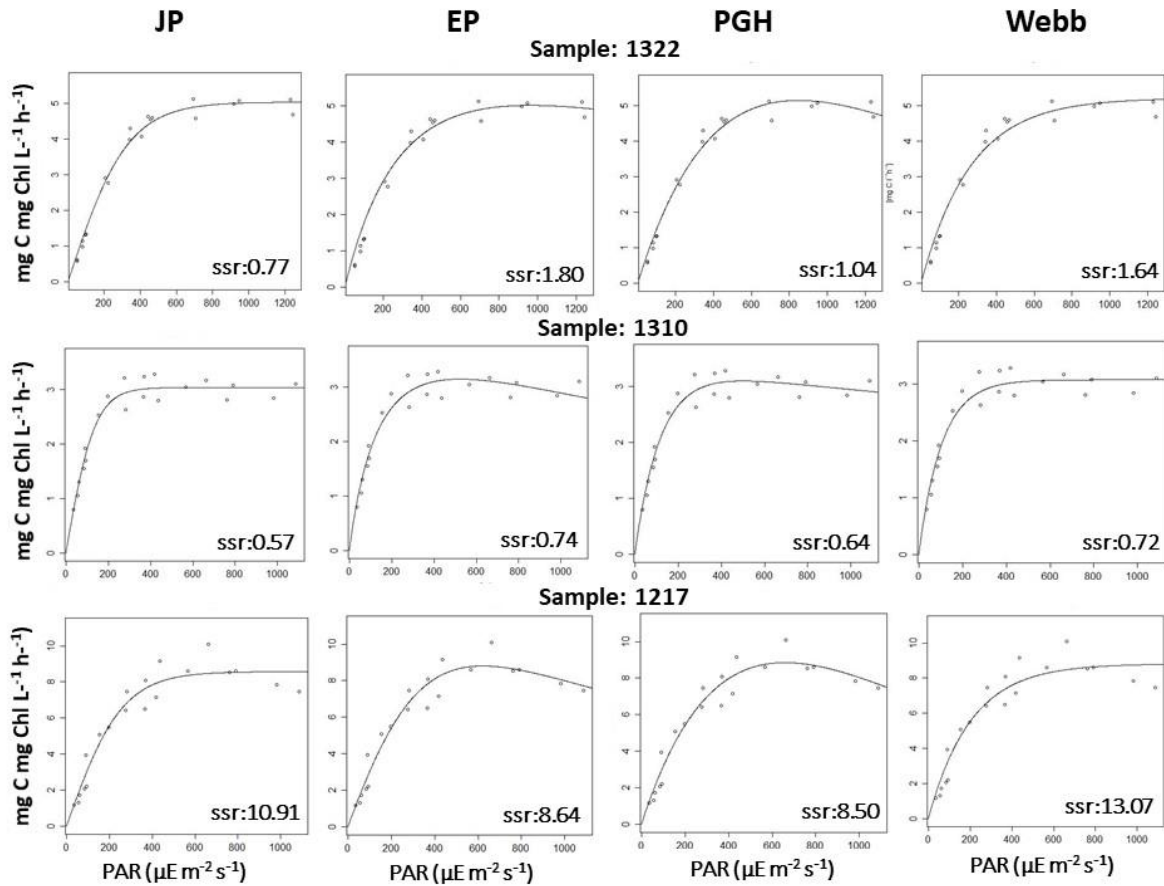
7

8

9

Figure 6. Four models were applied to the data; two without photo-inhibition (JP and Webb) and two models with photo-inhibition (EP and PGH), where ssr indicates the smallest squared sum of residuals. Examples of PE-curves are shown for three dates: July 15 2013 (1322), April 9 2013 (1310) and June19 2012 (1217).

1
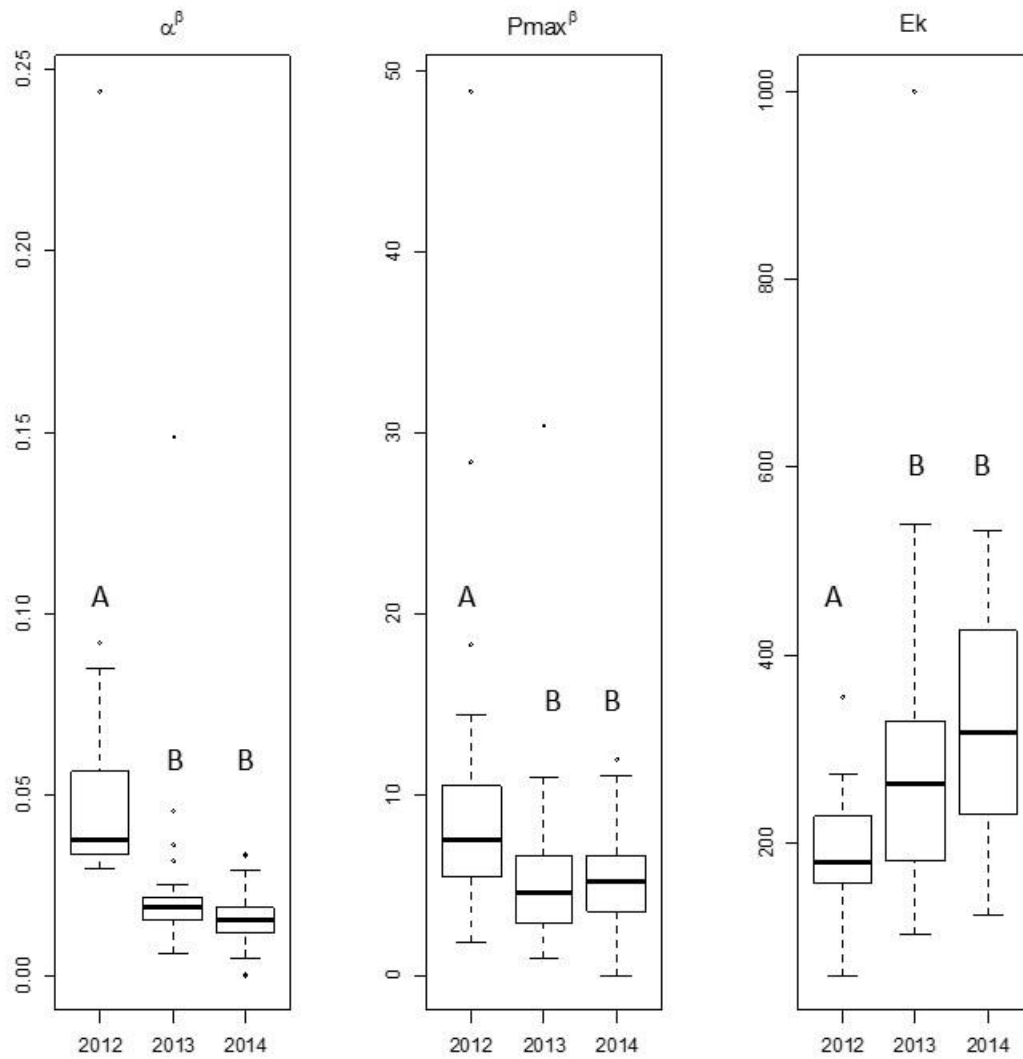
Figure 7. Box-whisker plots of the variation per year in estimates for α^B (mg C (mg Chl)$^{-1}$ h^{-1} (μmol m^{-2} s^{-1})$^{-1}$), P^B_{max} (mg C (mg Chl)$^{-1}$ h^{-1}) and E_k (μmol m^{-2} s^{-1}) using PE-curve fits from model JP. Different letters indicate significant difference (p < 0.05) between years.

5
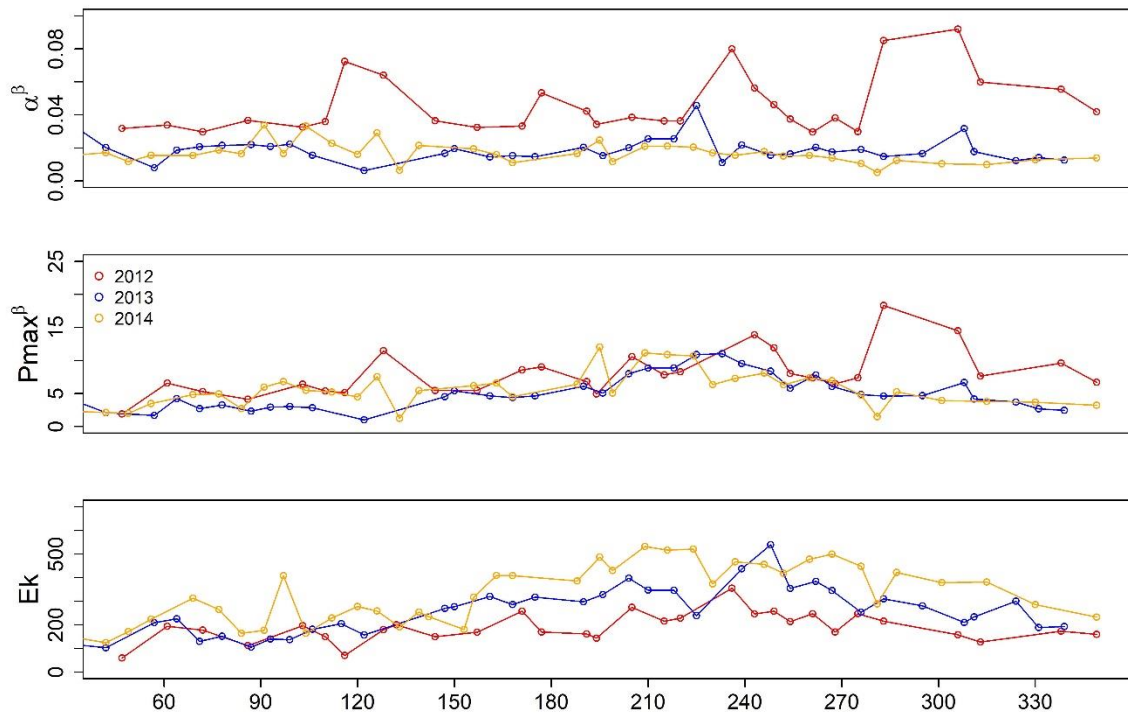
1

2 *Figure 8. Chlorophyll-a normalised photosynthetic parameters α^B (mg C (mg Chl)$^{-1}$ h^{-1}*

3 *(μmol photons m^{-2} s^{-1})$^{-1}$) and P^B_{max} (mg C (mg Chl) $^{-1}$ h^{-1}) as well as E_k (μmol photons m^{-2} s^{-}*

4 *^{1}), as estimated by means of the JP model at the Marsdiep jetty in the years 2012, 2013 and*

5 *2014. Note that outliers (see material & methods) were removed for better visualisation*

6 *of the seasonal pattern of photosynthetic parameters.*
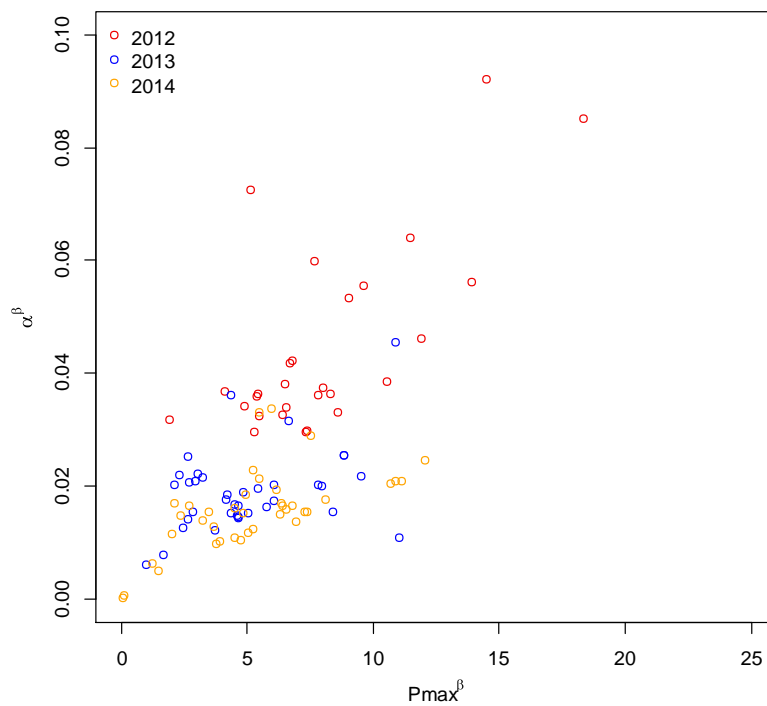
1

2   *Figure 9. Relationship between α^B and P^B_{max} (as estimated by means of the JP model) at the*

3   *Marsdiep jetty in the years 2012, 2013 and 2014. Outliers for α^B and P^B_{max} were omitted for*
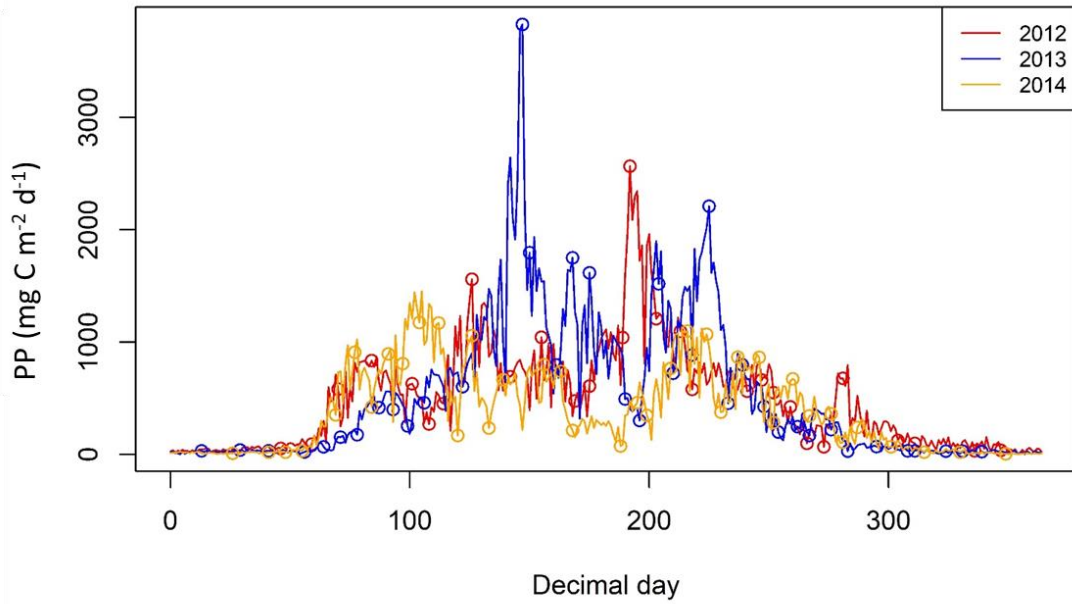
4   *clarity (see material & methods).*
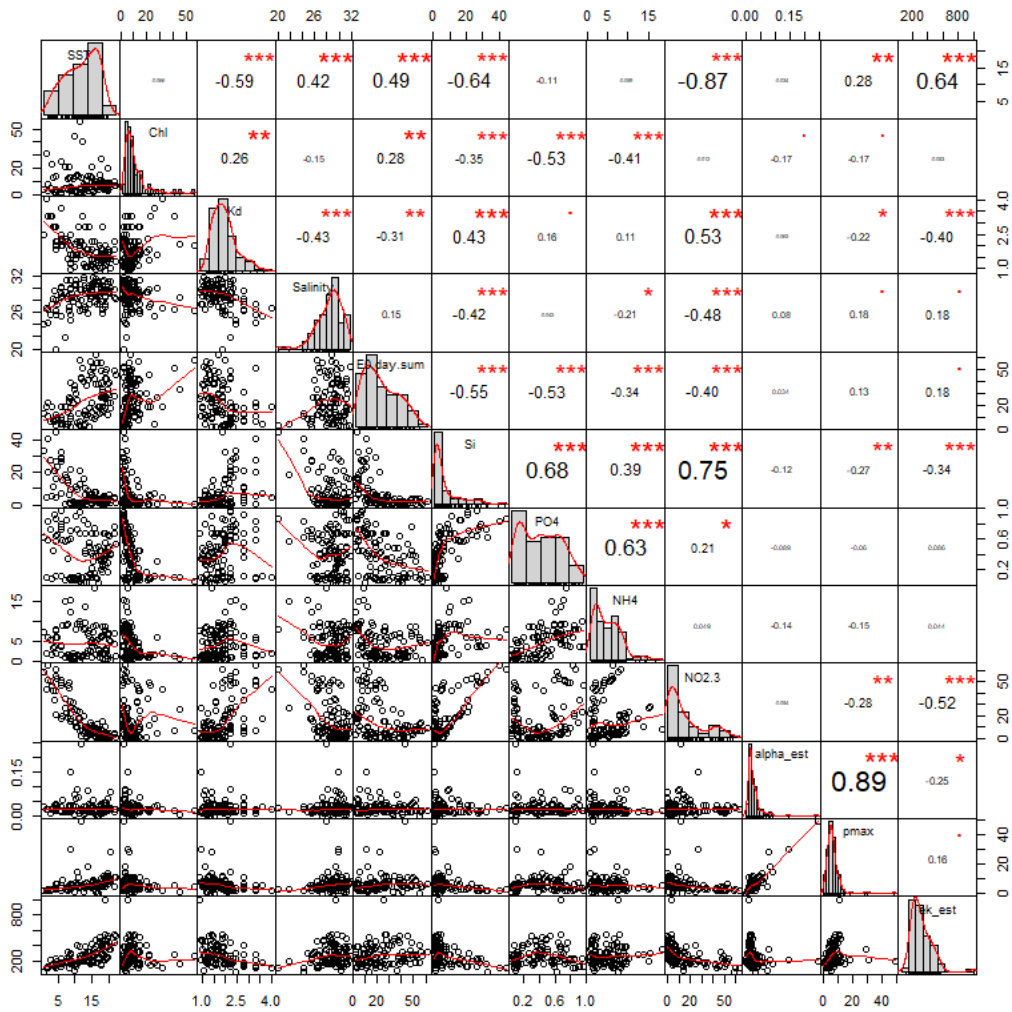
Figure 10. Correlations between the environmental variables measured at the Marsdiep jetty in the years 2012, 2013 and 2014 and the photosynthetic parameters α^B, P^B_{max} and E_k.

1

2 *Figure 11. The daily estimates (open circles) and the integrated production for the days in*

3 *between the sampling dates (see material and methods section for details of calculation*

4 *and integration procedure) for column integrated primary production at the Marsdiep*

5 *jetty in the years 2012, 2013 and 2014. The estimates were made using the curve fit from*

6 *the JP model.*

7
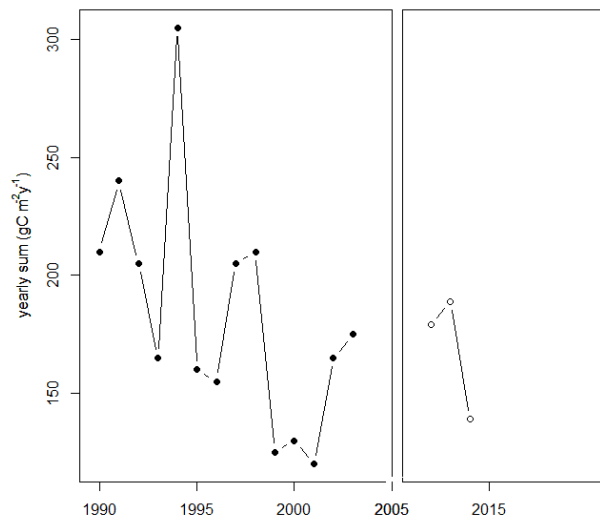
1

2   *Figure 12. The long-term trend in annual planktonic primary production (g C m⁻² y⁻¹) at*

3   *the Marsdiep jetty for the period 1990-2003 (closed circles: from Philippart et al. 2007)*

4   *and for the years 2012, 2013 and 2014 (open circles: this study).*

5

Supplementary material:
Planktonic primary production in the western Dutch Wadden Sea

1. Seasonality in nutrient concentrations
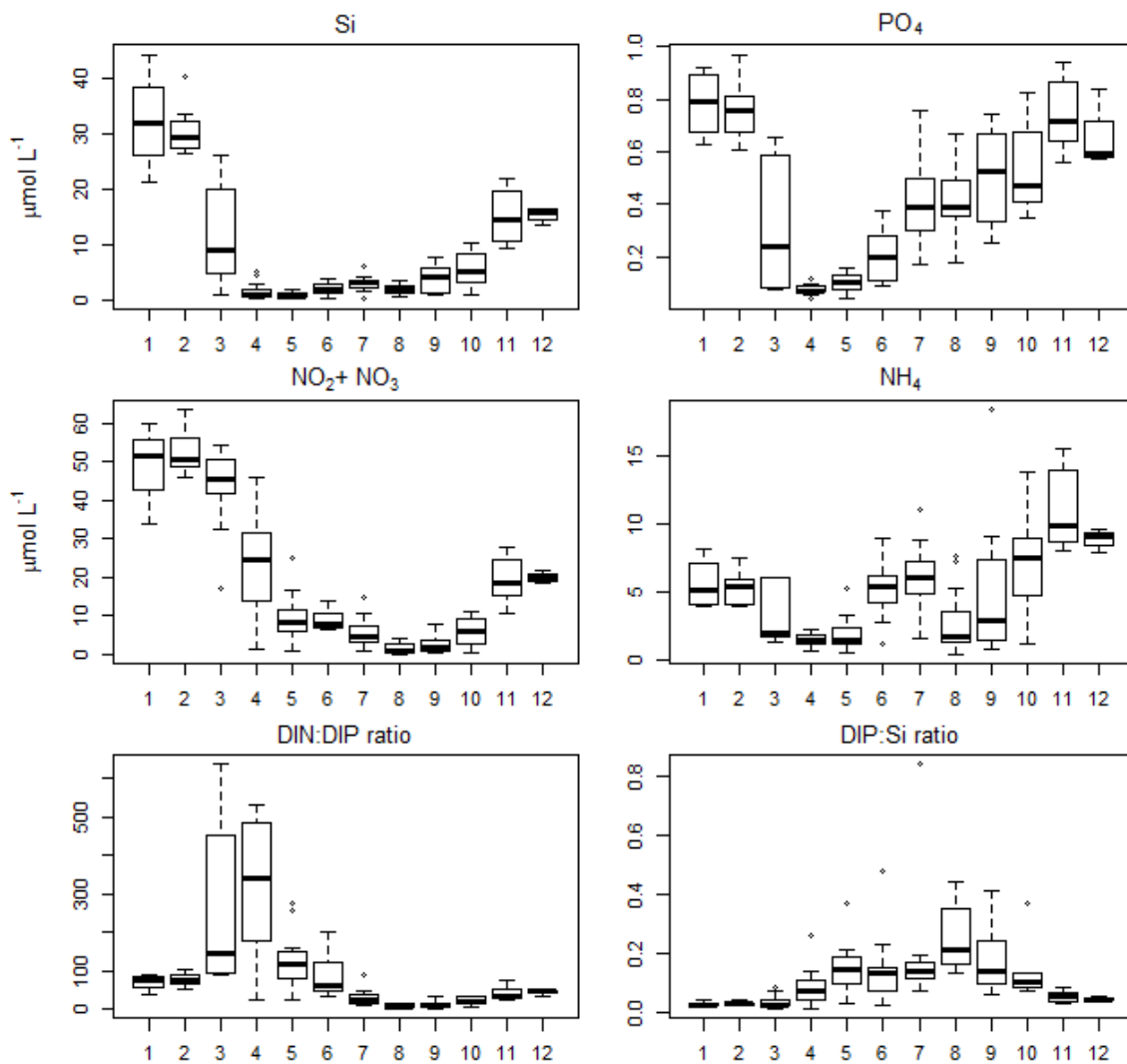

Figure S1. Monthly concentration of dissolved silicate (Si), dissolved inorganic nitrogen (DIN), phosphate (DIP), all in µmol L^{-1} and DIN:DIP and DIP:Si ratios for the Marsdiep jetty in the years 2012, 2013 and 2014.

Supplementary material:
Planktonic primary production in the western Dutch Wadden Sea

2. Analyses of the relation of photosynthetic parameters P^B_{max} and E_k to environmental variables.

Table S2A. Model outcomes of relationships between P^B_{max} (as estimated by means of the JP model) and environmental variables. Model 1) all significantly correlated variables, model 2-4) removal of variables. For all models, p values were <0.0001. Models were constructed, excluding year as a factor (model a) or including year as a factor (model b). Outliers (n=3) values were removed (model c). The explained variance of the model (R^2), the Akaike information criterion (AIC), the test value (F) and the two degrees of freedom are given (df). The p-values of the models were always <0.0001.

Model	description	R^2	AIC	F	(df)
Excluding year effect					
1a	$P^B_{max} \sim SST+NO_{2+3}+K_d+Si$	0.10	690	2.70	(4, 102)
2a	$P^B_{max} \sim SST+K_d+Si$	0.10	689	3.59	(3, 103)
3a	$P^B_{max} \sim SST+ K_d$	0.08	**688**	4.82	(2, 104)
4a	$P^B_{max} \sim SST$	0.07	**687**	8.78	(1, 105)
Including year effect					
1b	$P^B_{max} \sim SST+NO_{2+3}+K_d+Si+\underline{year}$	0.21	680	4.36	(6, 100)
2b	$P^B_{max} \sim SST+K_d+Si+\underline{year}$	0.20	679	5.10	(5, 101)
3b	$P^B_{max} \sim SST+K_d+\underline{year}$	0.20	678	6.26	(4, 102)
4b	$P^B_{max} \sim SST+\underline{year}$	0.20	**676**	8.39	(3, 103)
After removing outliers					
1c	$P^B_{max} \sim SST+NO_{2+3}+K_d+Si$	0.30	513	8.35	(5, 98)
2c	$P^B_{max} \sim SST+K_d+Si$	0.28	511	13.09	(3, 100)
3c	$P^B_{max} \sim SST+ K_d$	0.28	509	19.78	(2, 101)
4c	$P^B_{max} \sim SST$	0.28	**507**	39.36	(1, 102)

Supplementary material:
Planktonic primary production in the western Dutch Wadden Sea

Table S2B. Model outcomes of relationships between E_k (JP model) and environmental variables (n=107). Model 1) all significantly correlated variables, model 2-3) stepwise removal of variables. Models were constructed excluding year as a factor or including year as a factor. The explained variance of the model (R^2), the Akaike information criterion (AIC), the test value (F) and the two degrees of freedom are given (df). The p-values of the models were always <0.0001.

Model	description	R^2	AIC	F	(df)
Excluding year effect					
1a	$E_k \sim SST+NO_{2+3}+K_d+Si$	0.42	1307	18.26	(4, 102)
2a	$E_k \sim SST+Kd$	0.41	1305	35.85	(2, 104)
3a	$E_k \sim SST$	0.41	**1303**	72.16	(1, 105)
Including year effect					
1b	$E_k \sim SST+NO_{2+3}+K_d+Si +year$	0.57	1279	21.90	(6, 100)
2b	$E_k \sim SST+Kd+year$	0.57	**1276**	33.16	(4, 102)
3b	$E_k \sim SST+ year$	0.56	**1275**	44.25	(3, 103)

Note: removing one outlier (E_k=1000 µmol photons m^{-2} s^{-1}) resulted in a much better prediction of E_k. A model without year: R^2=0.47, AIC=1245, with year as a factor: R^2=0.67, AIC=1198.

Supplementary material:
Planktonic primary production in the western Dutch Wadden Sea

3. Calculating production rates in Philippart et al. (2007).

In the current study, calculated annual production rates were compared to previously reported rates (Philippart et al. 2007). However, there were differences between the previous and current study in how the production rates were calculated. In this paragraph, the differences in calculation methods used as well as the consequences for the rates are discussed. The methods used in the current study are described in the material & methods section. Philippart et al. (2007) measured carbon fixation rates at one fixed light intensity of approximately 400 µmol photons m^{-2} s^{-1} (PAR). To calculate daily production values, a linear relation between light and fixation rate was assumed. Because the fixation rate increases with light until light intensities become saturating, assuming a linear relation between light and carbon fixation rates result in an overestimation of daily production rates if *in situ* light conditions become saturated. And, the authors calculated the vertical light attenuation based on an empirical relation with Secchi disc depth from a different system (the Eastern and Western Scheldt estuaries, The Netherlands). Comparing the attenuation coefficient based on this relation and the relation used in the current study, which is based on an empirical relation at the sampling location, it is seen that the attenuation in Philippart et al. (2007) is on average 27% higher. This means that the potential overestimation due to a linear relation with light in the calculation of the carbon fixation rate could be compensated for by a reduction in the water column production due to the higher attenuation of light in the water column. To investigate the potential errors made in calculating production rates by Philippart et al. (2007), the daily column production rates were calculated for the years 2012-2014 using the method described in that paper (Figure S3). The estimates for the daily column production of the current study were on average 8% higher.
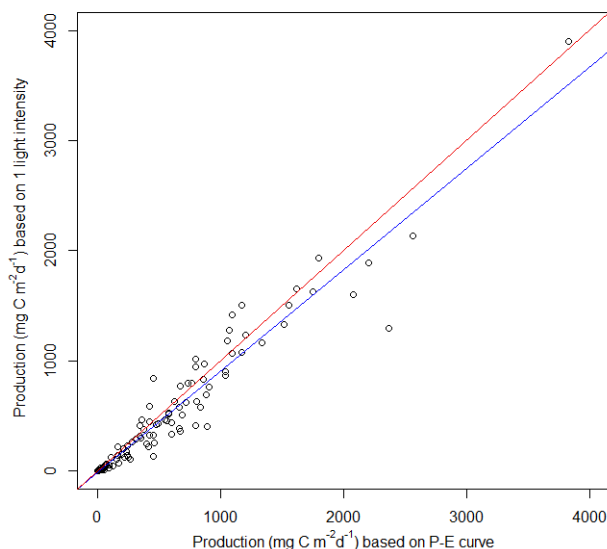

Figure S3. The daily column production in mg C m^{-2} d^{-1} for the period 2012-2014 based on the methods described in the current study and calculated based on a method described by Philippart et al. 2007. The red line indicates the line y=x, the blue line the regression line (y= -16.4 ± 21.9 (n.s.) + 0.92 ± 0.02x (p<0.0001), R^2=0.93).

Supplementary material:
Planktonic primary production in the western Dutch Wadden Sea

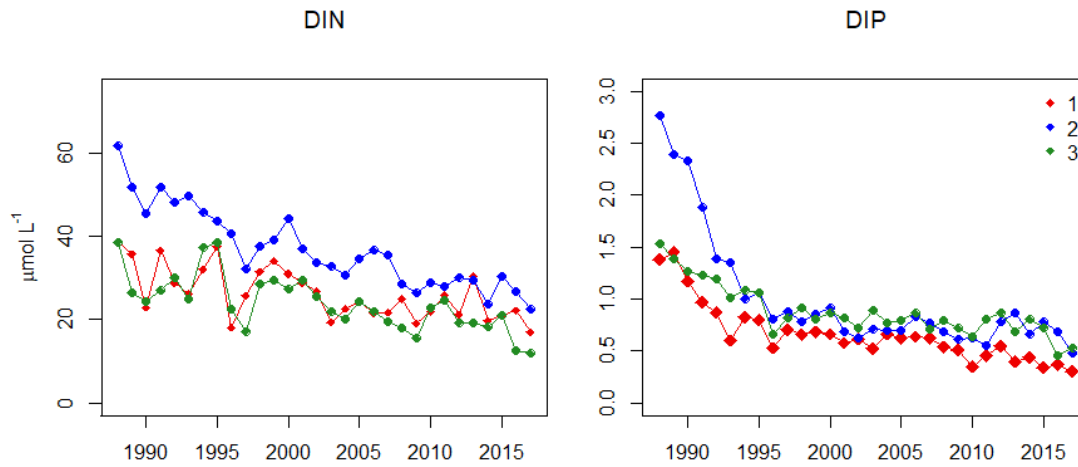## 4. Long-term nutrient concentrations in the Dutch coastal zone.

Figure S4A. The long-term year average concentrations (1988-2017) for dissolved inorganic nitrogen (N-DIN) and inorganic phosphate (P-DIP) in µmol L^{-1}, for three stations along the Dutch coastal zone. Station1: Marsdiep North, station 2: Noordwijk 2km off the coast, station 3: Walcheren 2 km off the coast. Data was collected and provided by Rijkswaterstaat (www.waterinfo.nl).
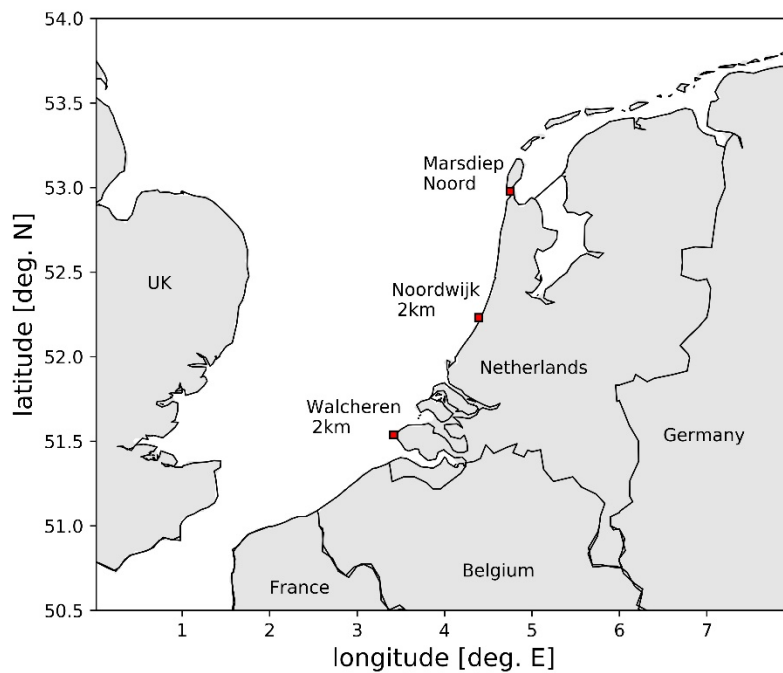

Figure S4B. Map showing the three sampling locations.